

# LIGHT ELEMENTS AND COSMIC RAYS IN THE EARLY GALAXY

REUVEN RAMATY

Laboratory for High Energy Astrophysics, Goddard Space Flight Center, Greenbelt, MD 20771

BENZION KOZLOVSKY

Sackler Faculty of Exact Science, Tel Aviv University, Ramat Aviv, Tel Aviv 69978, Israel

RICHARD E. LINGENFELTER

Center for Astrophysics and Space Sciences, University of California at San Diego, 9500 Gilman Drive, La Jolla, CA 92093

AND

HUBERT REEVES

CEA, DSM, DAPNIA, Service d'Astrophysique, 91191 Gif-sur-Yvette, France

*Received 1997 April 9; accepted 1997 June 5*

## ABSTRACT

Observations of Be and B in low-metallicity halo stars formed during the first  $10^9$  yr of Galactic evolution show that cosmic-ray acceleration must have taken place in the early Galaxy. The observed abundances of these elements relative to Fe, which, in the early Galaxy, is almost exclusively produced in Type II supernovae, strongly suggest that the cosmic-ray acceleration is also related to such supernovae with the particles being accelerated out of freshly nucleosynthesized matter before it mixes into the ambient, essentially nonmetallic interstellar medium. The observed abundances require that about  $3 \times 10^{49}$  to  $2 \times 10^{50}$  ergs per Type II supernova be imparted to these metallic cosmic rays, depending on whether or not H and He are accelerated along with the metals. The current data, however, are not sufficient to decide whether these cosmic rays are predominantly low energy or high energy. But, in any case, arguments of energetics imply a hard-energy spectrum extending up in energy to at least 50 MeV nucleon<sup>-1</sup>. This rules out Be and B production by supernova ejecta without further acceleration. In addition to production by cosmic rays, there must also be significant <sup>11</sup>B production by neutrinos. This argument is driven by the observed <sup>11</sup>B/<sup>10</sup>B ratio in meteorites that is very difficult to reproduce by cosmic-ray interactions. Observations of <sup>6</sup>Li and Li in the early Galaxy provide information on the acceleration of nonmetallic cosmic rays out of the interstellar medium.

*Subject headings:* acceleration of particles — cosmic rays — Galaxy: abundances —  
 Galaxy: evolution — nuclear reactions, nucleosynthesis, abundances

## 1. INTRODUCTION

It has been known for over two decades that cosmic-ray interactions in the interstellar medium could have an important role in the origin of the light elements, Li, Be, and B, hereafter LiBeB (Reeves, Fowler, & Hoyle 1970; Reeves 1994). Even though the LiBeB isotopes are not entirely cosmic-ray produced, detailed investigations of the cosmic-ray production can set very important constraints on the other LiBeB sources, as well as on the sources of the cosmic rays themselves. The bulk of the <sup>6</sup>Li, <sup>9</sup>Be, and <sup>10</sup>B are expected to be produced by cosmic rays, and here we refer to a variety of accelerated particle populations, not just the observed Galactic cosmic rays. However, about 10% of the <sup>7</sup>Li results from nucleosynthesis in the big bang (e.g., Spite & Spite 1993), and nucleosynthesis in a variety of Galactic objects, including Type II supernovae (Woosley et al. 1990), novae (Hernanz et al. 1996), and giant stars (Plez, Smith, & Lambert 1993; Wallerstein & Morrell 1994), can produce a large fraction of the remaining 90%. Core collapse supernovae (Types II, Ib, etc., hereafter referred to simply as SNII) can also contribute to <sup>11</sup>B production via <sup>12</sup>C spallation by neutrinos (Woosley et al. 1990).

The implications of the discovery of 3–7 MeV gamma-ray emission from the Orion star formation region on LiBeB origin (Bloemen et al. 1994) were first pointed out by Cassé, Lehoucq, & Vangioni-Flam (1995). The observed emission is most likely nuclear line emission resulting from

de-excitations in <sup>12</sup>C and <sup>16</sup>O. Such line emission can be produced only by cosmic-ray interactions. However, since irradiation of the Orion region by the standard Galactic cosmic rays (GCRs), which accounts for the greater than 30 MeV gamma-ray emission observed from the Orion cloud complex (Digel, Hunter, & Mukherjee 1995), underproduces the observed line emission by at least 3 orders of magnitude, the gamma-ray line production must be predominantly a low-energy cosmic-ray (LECR) phenomenon, requiring very large LECR fluxes in Orion (see Bloemen et al. 1994 and Ramaty 1996 for review). While the original Orion gamma-ray line data (Bloemen et al. 1994) were consistent (Ramaty, Kozlovsky, & Lingenfelter 1995; Cowsik & Friedlander 1995) with a LECR composition that included protons,  $\alpha$ -particles, and metals in proportions similar to those inferred for the sources of the GCRs (Lund 1989; Engelmann et al. 1990), the current data (Bloemen et al. 1997), based on more extended observations, seem to require LECRs depleted in protons and  $\alpha$ -particles (Kozlovsky, Ramaty, & Lingenfelter 1997). In addition, upper limits on the 1–3 MeV emission from Orion set constraints on the accelerated Ne-Fe abundances relative to those of C and O in these low-energy particles (e.g., Ramaty 1996).

There are two issues that suggested a connection between the Orion gamma-ray line observations and the LiBeB origin: the B isotopic ratio and the constancy of the B/Fe

and Be/Fe abundance ratios as functions of the Galactic metallicity. Hereafter, we shall use ratios of chemical or isotopic symbols to denote ratios by number of the respective elements or isotopes in various sites.

Concerning the B isotopic ratio,  $^{11}\text{B}/^{10}\text{B}$  in meteorites (Chaussidon & Robert 1995) and in the interstellar medium (Federman et al. 1996) exceeds the value calculated for production by the GCRs. The fact that  $^{11}\text{B}/^{10}\text{B}$  calculated for the LECRs exceeds the GCR value has been a motivation for suggesting a close relationship between the Orion gamma-ray observations and the LiBeB origin (Cassé et al. 1995; Reeves & Prantzos 1995; Ramaty, Kozlovsky, & Lingenfelter 1996, hereafter RKL96; Vangioni-Flam et al. 1996). However, at least some of the excess  $^{11}\text{B}$  could be due to production by neutrinos in SNIIs (Woosley et al. 1990), and, as we shall show, LECR production of the entire  $^{11}\text{B}$  excess would impose extreme conditions on the spectrum of the LECRs.

A variety of observations (see Duncan et al. 1996, Casuso & Beckman 1997, and Lemoine et al. 1997 for summaries of the data) have shown that the abundance ratios Be/Fe and B/Fe are constant, independent of the metallicity  $Z/Z_{\odot}$  at least up to  $Z/Z_{\odot} \simeq 0.1$ , where  $Z/Z_{\odot} \equiv (\text{Fe}/\text{H})/(\text{Fe}/\text{H})_{\odot}$ , and  $(\text{Fe}/\text{H})/(\text{Fe}/\text{H})_{\odot}$  is the Fe abundance relative to its solar value. It was first pointed out by Duncan, Lambert, & Lemke (1992) that this constancy implies that the C, N, and O abundances in the cosmic rays, which produce the Be and B, must be high enough so that the bulk of the Be and B is produced by accelerated metals interacting with ambient H and He rather than by accelerated protons and  $\alpha$ -particles interacting with ambient metals (see also Prantzos 1993). This is because, in the cosmic rays, the metal abundances can remain constant, whereas in the ambient medium, they increase with metallicity. Since the metal abundances of the interstellar medium (ISM) in the early Galaxy were very low, this requires that the cosmic rays be accelerated from freshly nucleosynthesized matter before it mixes into the ISM. The fact that the LECRs in Orion appear to consist mostly of accelerated metals (C and O) has provided the other link between the Orion gamma-ray observations and the LiBeB production in the early Galaxy. In fact, in the model of Vangioni-Flam et al. (1996), it was assumed that the metallic cosmic rays in the early Galaxy are necessarily LECRs, an assumption that we shall relax in the present paper. The suppression of the accelerated Ne-Fe abundances in Orion has no implications for LiBeB production.

Since the extent of the LECR phenomenon in the Galaxy is not yet known (as yet, nuclear gamma-ray line emission has been reported only from Orion), and because it is more favorable energetically to produce the LiBeB with higher energy cosmic rays, we shall explore LiBeB production by cosmic rays with a variety of energy spectra and compositions. The first detailed calculations of LiBeB production were done by Menguzzi, Audouze, & Reeves (1971) and Mitler (1972). Most recently, the problem was considered by Fields, Olive, & Schramm (1994) for GCRs and RKL96 for LECRs, but there are no comprehensive calculations of LiBeB production that bridge these two regimes. Furthermore, for calculations of LiBeB production by high-energy cosmic rays interacting in a low-metallicity ambient medium, it is necessary to incorporate the nuclear reactions due to the secondary fast nuclei produced by the originally accelerated particles. The incorporation of these nuclear reactions is essential for the accurate calculation of elemen-

tal and isotopic ratios, most notably B/Be, which turns out to be one of the most important diagnostics of cosmic-ray and neutrino nucleosynthesis processes in the early Galaxy. Our calculations also use the most recent nuclear data. A copy of our FORTRAN code for the calculation of LiBeB production can be obtained upon request (send email to ramaty@pair.gsfc.nasa.gov).

The study of the LiBeB origin requires, in addition to accurate production calculations, a treatment of the Galactic evolution of the LiBeB abundances. In all the previous studies (e.g., Prantzos, Cassé, & Vangioni-Flam 1993; Vangioni-Flam et al. 1996; Casuso & Beckman 1997), the LiBeB evolution is tied to the general problem of Galactic evolution. However, as we shall see, the constancy of Be/Fe and B/Fe for  $Z/Z_{\odot} < 0.1$  will allow us to replace the evolution of Be/H and B/H with calculations of the total Galactic inventories of these elements by relating the production rates of Be and B to the well-known Fe production rate by SNIIs in this range of metallicities. In particular, we shall normalize the Be and B production to the energy in cosmic rays that is required per SNII to account for the observations. As we shall see, the energetic considerations serve as excellent criteria for the viability of the models. It is for this reason that our production calculations are set up in such a fashion that the relationship between isotope production and the required cosmic-ray energy content is clearly displayed.

In § 2, we present in detail the formalism of LiBeB production, including the two-step processes and updated cross sections. In § 3, we consider separately the evolution of Be, B, and Li. In the treatment of B, we discuss in detail the issue of  $^{11}\text{B}$  production by neutrinos in SNIIs, while in the treatment of Li, we investigate the implications of the  $^6\text{Li}$  observations of low-metallicity stars. In § 4, we briefly consider the issue of the gamma-ray line emission that accompanies the LiBeB production, and we present our conclusions in § 5. Preliminary presentations of part of the results of the current paper can be found in Ramaty et al. (1997a, 1997b).

## 2. LiBeB PRODUCTION

### 2.1. Formalism

We consider the production of LiBeB via both one-step and two-step processes. The one-step processes involve the interactions of  $^{12}\text{C}$ ,  $^{14}\text{N}$ , and  $^{16}\text{O}$  with protons and  $\alpha$ -particles, leading directly to any one of the five isotopes  $^{11}\text{B}$ ,  $^{10}\text{B}$ ,  $^9\text{Be}$ ,  $^7\text{Li}$ , and  $^6\text{Li}$ . The two-step processes take into account the production of a secondary nucleus that can produce LiBeB also, for example,  $^{12}\text{C} \rightarrow ^{11}\text{B} \rightarrow ^9\text{Be}$ . We consider both reactions in which the projectiles are protons and  $\alpha$ -particles (hereafter direct reactions) and reactions in which the projectiles are  $^{12}\text{C}$ ,  $^{14}\text{N}$ , and  $^{16}\text{O}$  (hereafter inverse reactions). We take into account two-step processes only for the inverse reactions because in the direct reactions, the energies of the bulk of the secondary nuclei are too low to allow them to interact before they slow down because of Coulomb losses.

For the one-step processes, we consider the following reactions:  $^{12}\text{C}(p, x)\text{LiBeB}$ ,  $^{14}\text{N}(p, x)\text{LiBeB}$ , and  $^{16}\text{O}(p, x)\text{LiBeB}$ ; the corresponding reactions with  $\alpha$ -particles;  $^{13}\text{C}(p, x)^{10}\text{B}$ ,  $^{13}\text{C}(p, x)^9\text{Be}$ , and  $^{13}\text{C}(p, x)^6\text{Li}$ ; and  $^4\text{He}(\alpha, x)^7\text{Li}$  and  $^4\text{He}(\alpha, x)^6\text{Li}$ . We only consider stable isotopes, since the contributions of the radioactive isotopes are

included in the cross sections. Thus, the production of  $^{11}\text{B}$  includes  $^{11}\text{C}$ , that of  $^{10}\text{B}$  includes  $^{10}\text{C}$  and  $^{10}\text{Be}$ , and that of  $^7\text{Li}$  includes  $^7\text{Be}$ . For the reactions of  $^{12}\text{C}$ ,  $^{14}\text{N}$ , and  $^{16}\text{O}$  with protons, we used the cross sections of Read & Viola (1984) up to about 100 MeV nucleon $^{-1}$ . We continued these cross sections to higher energies using the measurements of W. R. Webber (1996, private communication) at 400 MeV nucleon $^{-1}$  and Webber, Kish, & Schreier (1990b) at 600 MeV nucleon $^{-1}$ , and we augmented our compilation at high energies with the data summarized by Read & Viola (1984) and Garcia-Munoz et al. (1987). The high-energy, Read & Viola (1984) data are generally in agreement with those of W. R. Webber (1996, private communication), except for Li production from  $^{14}\text{N}$ . For  $^7\text{Li}$ , the Webber data are higher, while for  $^6\text{Li}$ , they are lower, both by about

a factor of 2. We summarize these cross sections in Figure 1 (*left three panels*). Figure 1 also shows (*top left panel*) the cross sections for  $^{10}\text{B}$ ,  $^9\text{Be}$ , and  $^6\text{Li}$  from  $^{13}\text{C}$  by protons of energies less than about 15 MeV (Read & Viola 1984). The cross sections for the reactions of  $^{12}\text{C}$ ,  $^{14}\text{N}$ , and  $^{16}\text{O}$  with  $\alpha$ -particles are from Read & Viola (1984). We have adopted these cross sections (lower three right panels in Fig. 1) without further updates. The cross sections for  $^6\text{Li}$  and  $^7\text{Li}$  production in  $\alpha$ - $\alpha$  reactions (Fig. 1, *upper right panel*) are based on the compilation of Read & Viola (1984) and the recent reanalysis and measurements of Mercer, Austin, & Glagola (1997) and D. J. Mercer & S. M. Austin (1996, private communication). Since there are no  $\alpha$ - $\alpha$  measurements above 155 MeV nucleon $^{-1}$ , for  $^6\text{Li}$  we assumed that the cross section above 250 MeV nucleon $^{-1}$  is constant,

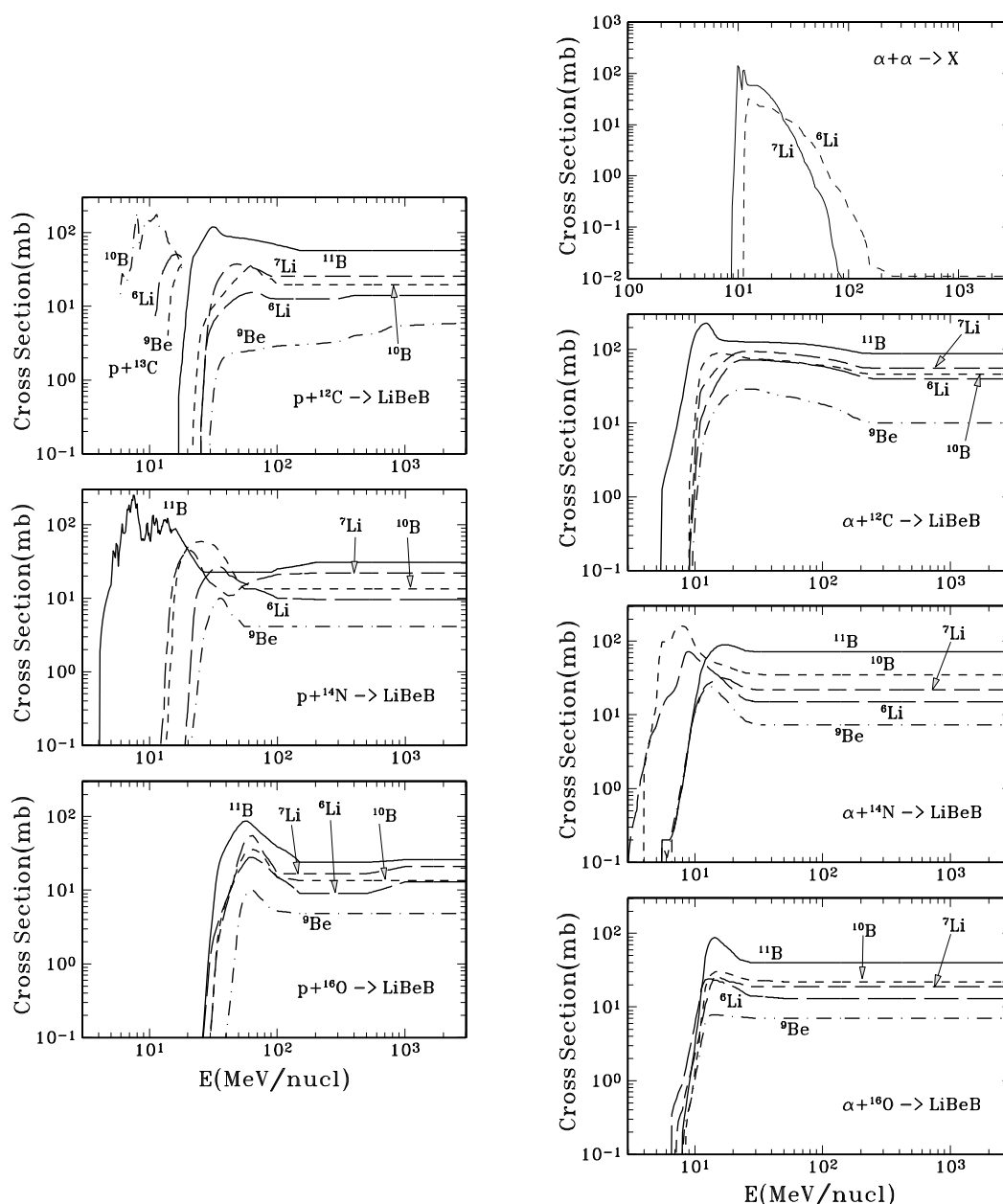


FIG. 1.—LiBeB production cross sections in proton and  $\alpha$ -particle interactions with He,  $^{12}\text{C}$ ,  $^{13}\text{C}$ ,  $^{14}\text{N}$ , and  $^{16}\text{O}$ . The data are from Read & Viola (1984), Webber et al. (1990b), W. R. Webber (1996, private communication), Mercer et al. (1997), and D. J. Mercer & S. M. Austin (1996, private communication).

equal to 0.01 mbarn, a value slightly lower than the measured cross section of 0.017 mbarn at 155 MeV nucleon<sup>-1</sup>. The measurements for <sup>7</sup>Li revealed only an upper limit at 155 MeV nucleon<sup>-1</sup> (<0.007 mbarn). This upper limit appears to be consistent with the two-body nature of <sup>7</sup>Li production. We have assumed that the <sup>7</sup>Li production cross section decreases exponentially at high energies. In § 2.2, we discuss the uncertainty introduced by these assumptions.

Starting with <sup>12</sup>C, <sup>14</sup>N, and <sup>16</sup>O, there are six two-step processes leading to <sup>11</sup>B, nine leading to <sup>10</sup>B, 12 leading to <sup>9</sup>Be, 15 leading to <sup>7</sup>Li, and 18 leading to <sup>6</sup>Li. Again, we only consider stable isotopes, since the contributions of the radioactive isotopes are included in the cross sections. To evaluate the contributions of these two-step processes to LiBeB production, in addition to the cross sections shown in Figure 1, we need cross sections for the reactions listed in Table 1. Since the two-step processes are important only at high energies, we have used high-energy cross section data, and we have assumed that the cross sections are independent of energy down to values near the reaction thresholds. These cross sections, from W. R. Webber (1996, private communication), Webber et al. (1990b), and from estimations based on nuclear systematics when no measurements are available, are also listed in Table 1, together with the reaction threshold energies.

We calculate LiBeB production by isotropic accelerated particles with given composition and energy spectrum interacting in an isotropic target region with given ambient medium composition. We consider a variety of compositions for both the accelerated particles and the ambient medium, including compositions characteristic of the early

Galaxy. We also consider a variety of accelerated particle energy spectra. We allow the primary and secondary fast particles, as well as the produced LiBeB, to either escape from, interact in, or slow down in the interaction region.

For the one-step processes, the yield of a particular LiBeB isotope  $k$  is given by

$$Q_k = \sum_{ij} \frac{n_j}{n_H} \int_0^\infty P_k(E_1, 0) \frac{\sigma_{ijk}(E_1) dE_1}{F_i(E_1)} \times \int_{E_1}^\infty q_i(E_0) P_i(E_0, E_1) dE_0, \quad (1)$$

where  $q_i$  is the source function of primary accelerated particles of type  $i$  (assumed to be time independent),  $P_i(E_0, E_1)$  is the survival probability of particles  $i$  against escape and nuclear destruction as they slow down from  $E_0$  to  $E_1$ ,  $F_i(E_1)$  is the energy-loss rate for these particles,  $\sigma_{ijk}$  is the cross section for producing isotope  $k$  by accelerated isotope  $i$  interacting with ambient isotope  $j$  of abundance  $n_j/n_H$ , and  $P_k(E_1, 0)$  is the survival probability of the LiBeB isotope  $k$  as it slows down from  $E_1$ . For the inverse reactions,  $P_k$  is calculated starting at  $E_1$  because, in these reactions, the isotope  $k$  is produced at nearly the same energy/nucleon as that of the projectile at interaction. This is not the case for the direct reactions. For these reactions, we set  $P_k = 1$  because the LiBeB isotopes are generally produced at sufficiently low energies to ensure survival. Equation (1) also can be used to calculate LiBeB production for time-dependent accelerated particle source functions. But in this case, both  $q_i$  and  $Q_k$  must be considered as total, time-integrated, particle yields.

In a neutral medium, the energy-loss rate  $F_i$ , measured in MeV nucleon<sup>-1</sup> cm<sup>2</sup>, is given by

$$F_i(E) = \left[ 1 + \left( 1.8 \frac{n_{He}}{n_H} \right) \right] \frac{Z_i^2(\text{eff})}{A_i} m_p \left( \frac{dE}{dx} \right)_{p,H}, \quad (2)$$

where  $m_p(dE/dx)_{p,H}$  is the energy-loss rate of accelerated protons in ambient H (Barkas & Berger 1964),  $Z_i(\text{eff}) = Z_i[1 - \exp(-137\beta/Z_i^{2/3})]$  is the equilibrium ionic charge (Pierce & Blann 1968),  $\beta$  is the particle velocity, and  $Z_i$  and  $A_i$  are the nuclear charge and mass for particle species  $i$ , respectively.

The survival probabilities are given by

$$P_i(E, E') = \exp \left\{ -[\sigma_{iH} + \sigma_{iHe}(n_{He}/n_H) + \sigma_e] \int_{E'}^E dE^*/F_i(E^*) \right\}, \quad (3)$$

where  $\sigma_{iH}$  and  $\sigma_{iHe}$  are the total mass changing cross sections for particle  $i$  in H and He, respectively (Webber, Kish, & Schrier 1990a), and  $\sigma_e^{-1}$  represents the number of atoms cm<sup>-2</sup> along the escape path of the particle from the interactions region. The approach embodied in equation (1) is equivalent to the standard leaky box model for Galactic cosmic-ray propagation, with  $\sigma_e^{-1} \simeq X_{\text{esc}}/m_p$ , where  $X_{\text{esc}}$  is the escape path of cosmic rays from the Galaxy.

As already mentioned, for the two-step processes, we only consider inverse reactions, i.e., interactions initiated by accelerated <sup>12</sup>C, <sup>14</sup>N, and <sup>16</sup>O. We have further simplified the treatment by explicitly considering only reactions on ambient H, with the contributions of the ambient He taken into account by increasing the cross sections by 15%. The

TABLE 1

REACTIONS, THRESHOLD ENERGIES, AND CROSS SECTIONS FOR THE TWO-STEP PROCESSES

Reaction	$E_{\text{th}}$ (MeV nucleon <sup>-1</sup> )	$\sigma$ (mbarn)
<sup>16</sup> O(p, x) <sup>15</sup> N.....	12.9	65.2 <sup>a</sup>
<sup>16</sup> O(p, x) <sup>14</sup> N.....	16.2	33.9 <sup>a</sup>
<sup>16</sup> O(p, x) <sup>13</sup> C.....	5.5	23.7 <sup>a</sup>
<sup>16</sup> O(p, x) <sup>12</sup> C.....	7.6	35 <sup>a</sup>
<sup>15</sup> N(p, x) <sup>11</sup> B.....	11.7	32.5 <sup>b</sup>
<sup>15</sup> N(p, x) <sup>10</sup> B.....	21.6	13.6 <sup>b</sup>
<sup>15</sup> N(p, x) <sup>9</sup> Be.....	22.7	7.5 <sup>b</sup>
<sup>15</sup> N(p, x) <sup>7</sup> Li.....	21.0	18.6 <sup>b</sup>
<sup>15</sup> N(p, x) <sup>6</sup> Li.....	26.3	10.5 <sup>b</sup>
<sup>14</sup> N(p, x) <sup>13</sup> C.....	8.9	17.1 <sup>a</sup>
<sup>14</sup> N(p, x) <sup>12</sup> C.....	5.1	53.2 <sup>a</sup>
<sup>13</sup> C(p, x) <sup>11</sup> B.....	14.2	50.6 <sup>c</sup>
<sup>13</sup> C(p, x) <sup>10</sup> B.....	4.4	29.2 <sup>c</sup>
<sup>13</sup> C(p, x) <sup>9</sup> Be.....	11.5	12.8 <sup>c</sup>
<sup>13</sup> C(p, x) <sup>7</sup> Li.....	21.8	9.1 <sup>c</sup>
<sup>13</sup> C(p, x) <sup>6</sup> Li.....	9.2	12.8 <sup>c</sup>
<sup>11</sup> B(p, x) <sup>10</sup> B.....	10.1	40.7 <sup>b</sup>
<sup>11</sup> B(p, x) <sup>9</sup> Be.....	11.3	14.6 <sup>b</sup>
<sup>11</sup> B(p, x) <sup>7</sup> Li.....	9.45	27.7 <sup>b</sup>
<sup>11</sup> B(p, x) <sup>6</sup> Li.....	13.3	6.3 <sup>b</sup>
<sup>10</sup> B(p, x) <sup>9</sup> Be.....	7.2	38.2 <sup>c</sup>
<sup>10</sup> B(p, x) <sup>7</sup> Li.....	0	3.5 <sup>c</sup>
<sup>10</sup> B(p, x) <sup>6</sup> Li.....	4.9	10.7 <sup>c</sup>
<sup>9</sup> Be(p, x) <sup>7</sup> Li.....	12.4	12.8 <sup>c</sup>
<sup>9</sup> Be(p, x) <sup>6</sup> Li.....	0	10 <sup>c</sup>
<sup>7</sup> Li(p, x) <sup>6</sup> Li.....	5.7	35.5 <sup>b</sup>

<sup>a</sup> Webber et al. 1990b, at 600 MeV nucleon<sup>-1</sup>.

<sup>b</sup> W. R. Webber 1996, private communication, at 400 MeV nucleon<sup>-1</sup>.

<sup>c</sup> Estimation.

yield of LiBeB isotope  $k$  is then given by

$$Q_k = \sum_{i=1}^3 \sum_{l=1}^{L(i,k)} \int_0^\infty dE_2 P_k(E_2, 0) \frac{\sigma_{ik}(E_2)}{F_i(E_2)} \times \int_{E_2}^\infty dE_1 P_l(E_1, E_2) \frac{\sigma_{il}(E_1)}{F_i(E_1)} \int_{E_1}^\infty dE_0 q_i(E_0) P_i(E_0, E_1), \quad (4)$$

where the index  $i$  denotes the primary  $^{12}\text{C}$ ,  $^{14}\text{N}$ , and  $^{16}\text{O}$ , and the index  $l$  runs over the intermediate nuclei whose number depends on  $i$  and  $k$ . Note that for  $^{11}\text{B}$  production,  $i$  runs over only  $^{14}\text{N}$  and  $^{16}\text{O}$  because there are no intermediate nuclei leading to  $^{11}\text{B}$  from  $^{12}\text{C}$ .

For time-independent accelerated particle source functions, the power in the accelerated particles that produce the LiBeB is given by

$$\dot{W} = \sum_i A_i \int_0^\infty E q_i(E) dE. \quad (5)$$

Equation (5) is also valid for time-dependent source functions. In this case,  $\dot{W}$  should be replaced by  $W$ , the total energy contained in the accelerated particles, and  $q_i$  by the total number of source particles.

The assumed compositions are summarized in Table 2. For the LiBeB production, we only consider nuclei up to and including  $^{16}\text{O}$ . We show the  $^{56}\text{Fe}$  abundances to indicate that in the calculations of  $\dot{W}$  (eq. [5]), we also take into account the energy contained in nuclei heavier than  $^{16}\text{O}$ . For the ambient medium composition (row 1), we use solar abundances (Anders & Grevesse 1989) scaled with metallicity,  $Z/Z_\odot$ , where  $Z/Z_\odot \equiv (\text{Fe}/\text{H})/(\text{Fe}/\text{H})_\odot$ , and  $(\text{Fe}/\text{H})/(\text{Fe}/\text{H})_\odot$  is the Fe abundance relative to its solar value. We shall use chemical or isotopic symbols to denote the Galactic inventories, i.e., the total number of atoms in the Galaxy (§ 3), of the respective elements or isotopes. Ratios of chemical or isotopic symbols, therefore, denote abundance ratios by number. For  $^{12}\text{C}$  and heavier nuclei, the ambient abundances are scaled with  $Z/Z_\odot$ ; the  $^4\text{He}$  abundance is scaled with a slowly varying function  $f$ , ranging from 1 at  $Z/Z_\odot = 1$  to 0.075 at  $Z/Z_\odot = 0.001$ , to take into account the difference between the solar and the early Galactic He abundance (e.g., Reeves 1994).

For the accelerated particle compositions we use the following:

1. SSz, identical to the ambient abundances (row 1): This would be the composition if the accelerated particles were accelerated directly out of the ISM.

2. CRS, current epoch cosmic-ray source abundances (Engelmann et al. 1990; Lund 1989; row 2): We take this composition independent of metallicity since the case in

which the cosmic rays would be accelerated from the ISM is already represented by SSz.

3. SNII, ejecta of Type II supernovae (12–40  $M_\odot$  progenitors; Woosley & Weaver 1995) averaged over an initial mass function (IMF) proportional to  $m^{-2.5}$  (e.g., Silk 1995) shown at four values of  $Z/Z_\odot$  (rows 4–7): These compositions would be appropriate if the accelerated particles were accelerated directly from the ejecta of such supernovae. We see that the SNII compositions are not strongly dependent on metallicity and that they are not too different from the CRS composition, except that they are less abundant in  $^{12}\text{C}$  and protons relative to  $^{16}\text{O}$ . However, it may not be possible to accelerate the freshly nucleosynthesized matter by the forward SNII shock, since this shock is probably formed ahead of the region containing the bulk of this matter.

4. SNII<sub>metal</sub>, identical to SNII, but with H = He = 0: This composition would be appropriate if the accelerated particles were accelerated by the reverse SNII shock from freshly nucleosynthesized matter, containing essentially no H and He, or by the forward shock from high-velocity grains of the more refractory ejecta that penetrate the slower shock. In either case, we would expect that significantly more energy would eventually go into H and He accelerated from the ISM by the forward shock.

5. CRS<sub>metal</sub>, identical to CRS, but with H = He = 0: This composition would be appropriate if the bulk of the C and O in the cosmic rays was accelerated from the presupernova winds of Wolf-Rayet stars (Meyer, Drury, & Ellison 1997) that do not contain much H and He. Most of this acceleration should be due to the forward supernova shock. However, the frequency of SNIIs from the very massive stellar progenitors that lead to the Wolf-Rayet stage is much lower than that of all Type II supernovae.

For the accelerated particle energy spectra, we assume the following:

1. Energy spectra resulting from shock acceleration (e.g., Ellison & Ramaty 1985),

$$q(E) \propto \frac{p^{-s}}{\beta} e^{-E/E_0}, \quad (6)$$

where  $p$  and  $E$  are particle momentum and kinetic energy, respectively, both per nucleon,  $c\beta$  is particle velocity, and  $E_0$  is a parameter that takes into account the possibility that the particle spectrum is cut off at high energies. We perform calculations for a variety of values for  $s$ . For  $s < 3$ ,  $\dot{W}$  given by equation (5) remains finite as  $E \rightarrow 0$ . For larger  $s$ , a low-energy cutoff must be imposed to keep  $\dot{W}$  finite. We set this cutoff at 1 MeV nucleon $^{-1}$  for all values of  $s$ .

TABLE 2  
ACCELERATED PARTICLE ABUNDANCES

Composition	H	$^4\text{He}$	$^{12}\text{C}$	$^{13}\text{C}$	$^{14}\text{N}$	$^{16}\text{O}$	$^{56}\text{Fe}$
Ambient Medium = SSz.....	1180	118 $f$	0.42 $Z/Z_\odot$	0.005 $Z/Z_\odot$	0.13 $Z/Z_\odot$	$Z/Z_\odot$	0.038 $Z/Z_\odot$
CRS.....	174	24	0.81	0.009	0.048	1	0.19
SNII:							
$Z/Z_\odot = 1$ .....	86	18	0.18	0.001	0.05	1	0.021
$Z/Z_\odot = 0.1$ .....	94	19	0.19	0.0001	0.005	1	0.024
$Z/Z_\odot = 0.01$ .....	100	19	0.19	0.00001	0.0006	1	0.027
$Z/Z_\odot = 0.001$ .....	120	22	0.21	0.00001	0.0001	1	0.026
SNII <sub>metal</sub> .....	0	0	<sup>a</sup>	<sup>a</sup>	<sup>a</sup>	<sup>a</sup>	<sup>a</sup>
CRS <sub>metal</sub> .....	0	0	0.81	0.009	0.048	1	0.19

<sup>a</sup> Identical to SNII.

2. A flat spectrum below a cutoff energy  $E_0$  changing to a steep power law at higher energies,

$$q_i(E) \propto \text{const for } E < E_0; \quad q_i(E) \propto E^{-10} \text{ for } E \geq E_0. \quad (7)$$

This spectrum was used in previous studies of gamma-ray line and LiBeB production (Cassé et al. 1995; RKL96). We employ this spectrum in the present paper as well, in order to make comparisons with the previous studies, but, more importantly, as we shall see below, with such a spectrum it is possible to produce a sufficiently high boron isotopic ratio  $[Q(^{11}\text{B})/Q(^{10}\text{B})]$  to account for the meteoritic observations (Chaussidon & Robert 1995).

For both the shock spectrum (eq. [6]) and the flat spectrum (eq. [7]), we allow  $E_0$  to vary over a broad range, from 3 to  $10^4$  MeV nucleon $^{-1}$ . We also vary the spectral index  $s$ , from  $s = 2$ , valid for strong shocks, to  $s = 7$ , for which equation (6) yields in the nonrelativistic region a kinetic energy per nucleon spectrum with index 4.

## 2.2. Numerical Results

We display the numerical results for the various assumed accelerated particle abundances and energy spectra as functions of both the metallicity  $Z/Z_\odot$  and the spectral parameters  $E_0$  and  $s$  (eqs. [6] and [7]). In all cases, the ambient medium abundances are solar scaled with  $Z/Z_\odot$  for the metals and  $f$  for  $^4\text{He}$  (Table 2). For most of our results, we use  $s = 2.2$ , the derived cosmic-ray source spectral index (Engelmann et al. 1990).

In Figure 2, we show  $Q(\text{B})/Q(\text{Be})$  for three selected compositions as a function of  $Z/Z_\odot$  for  $E_0 = 10$  GeV nucleon $^{-1}$  and two values of  $X_{\text{esc}}$ , the escape path of cosmic rays from the Galaxy. The inclusion of the two-step processes lowers significantly this ratio, particularly when the inverse reactions dominate. For example, for the CRS composition (Fig. 2a) at  $Z/Z_\odot = 10^{-3}$ ,  $Q(\text{B})/Q(\text{Be})$  is lowered by about 50%. We also see that for this composition without the inclusion of the two-step processes,  $Q(\text{B})/Q(\text{Be})$  decreases with increasing  $Z/Z_\odot$ . This variation, however, disappears when the two-step processes are included. If only the one-step processes are taken into account,  $Q(\text{B})/Q(\text{Be})$  is higher for the inverse reactions than for the direct reactions, mainly because of nuclear breakup that causes the B and Be to be produced, on average, at lower accelerated particle energies, where the cross sections and threshold energies favor B over Be. But when the two-step reactions are included, the nuclear breakup is compensated by the products of the breakup that favor Be. For the SN<sub>metal</sub> composition (Fig. 2b), the inverse reactions dominate at all metallicities. Hence, the two-step processes are important, and  $Q(\text{B})/Q(\text{Be})$  shows no variation with metallicity. For the SSz composition (Fig. 2c),  $Q(\text{B})/Q(\text{Be})$  is essentially constant because the relative contributions of the direct and inverse reactions do not vary with metallicity. But because the direct reactions are quite dominant in this case, the two-step processes are not very important.

The lowest ratio,  $Q(\text{B})/Q(\text{Be}) \simeq 10$ , is achieved with the SNII<sub>metal</sub> composition with  $X_{\text{esc}} \rightarrow \infty$  (Fig. 2b, also with SNII not shown). This lower limit is higher than that suggested by Walker et al. (1993), who assumed a composition that contains no C and limited the accelerated particles to high energies. The results of Figure 2c can be compared with those of Fields et al. (1994, Fig. 8a), where  $Q(\text{B})/Q(\text{Be})$  was calculated for only one set of abundances for both the

accelerated particles and the ambient medium. The values of Fields et al. (1994) vary from about 12 to 10.5 as  $X_{\text{esc}}$  increases from 10 to 1000 g cm $^{-2}$ . Our values are somewhat higher, decreasing from about 13 to 12, because we use a higher C/O and slightly steeper accelerated particle spectrum. But, as we shall see (§ 3), the SSz composition is ruled out for B and Be by both energetic and evolutionary considerations. For the other compositions, the appropriate  $Q(\text{B})/Q(\text{Be})$  in the early Galaxy would be at least 14 without the inclusion of the two-step processes. The calculated lower limit on the cosmic-ray-produced  $Q(\text{B})/Q(\text{Be})$  is important for the determination of the contribution of neutrinos to B production in Type II supernovae (§ 3.2).

In Figures 3 and 4, we show  $Q(\text{B})/Q(\text{Be})$  as functions of  $E_0$ , for selected compositions, for  $X_{\text{esc}} = 10$  g cm $^{-2}$  and  $\infty$ ,

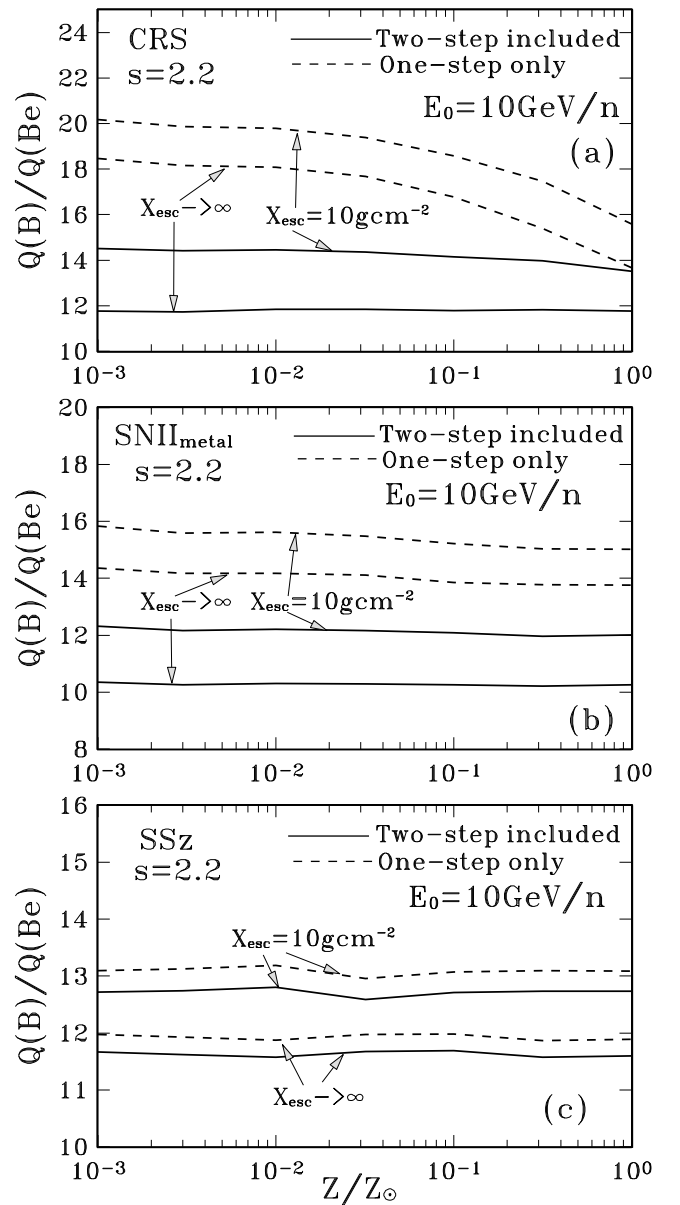


FIG. 2.—B/Be production ratios as functions of the ambient medium metallicity. The accelerated particle spectrum is from eq. (6). The three panels correspond to accelerated particle compositions given in Table 2.  $X_{\text{esc}} = 10$  g cm $^{-2}$  and  $X_{\text{esc}} \rightarrow \infty$  represent a leaky box and a closed Galaxy cosmic-ray propagation model, respectively.

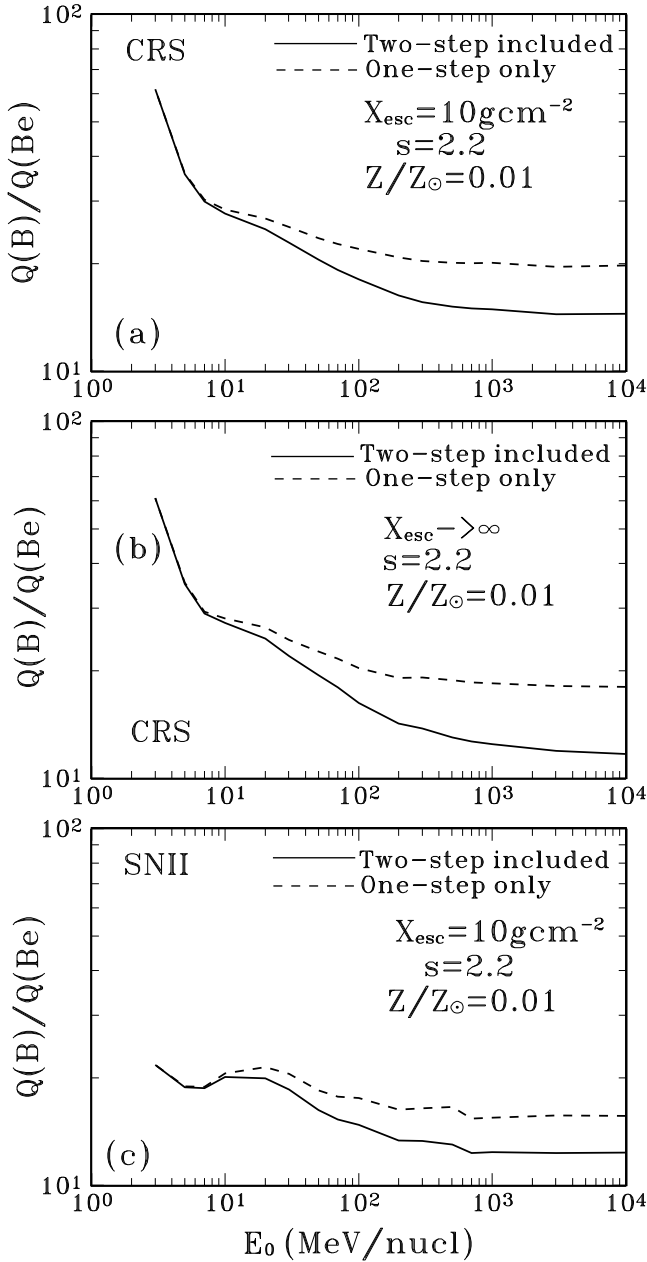


FIG. 3.—B/Be production ratios as a function of the characteristic energy  $E_0$  in eqs. (6) for a given ambient medium composition. Panels (a) and (b) are for the same accelerated particle composition but differ in the choice of  $X_{\text{esc}}$ , leaky box, and closed Galaxy. Panel (c) is for the SNII composition and the leaky box model.

and  $Z/Z_{\odot} = 0.01$ . We again note that  $Q(\text{B})/Q(\text{Be})$  is lowered significantly by the inclusion of the two-step processes, particularly at high energies. We also see that  $Q(\text{B})/Q(\text{Be})$  increases with decreasing  $E_0$  because of the higher cross sections and lower thresholds for B production than for Be production. The large  $Q(\text{B})/Q(\text{Be})$  at very low  $E_0$ , particularly for  $\text{CRS}_{\text{metal}}$ , is due to  $^{14}\text{N}$ . This becomes more clear in Figure 5, where we show  $Q(\text{B})/Q(\text{Be})$  resulting from the interactions of pure C, N, or O with an ambient medium at metallicity  $Z/Z_{\odot} = 0.01$ .

In Figure 6, we show  $Q(^{11}\text{B})/Q(^{10}\text{B})$  as a function of  $E_0$  for the same cases as considered in Figures 3 and 4. Hereafter, we only show results with the two-step processes

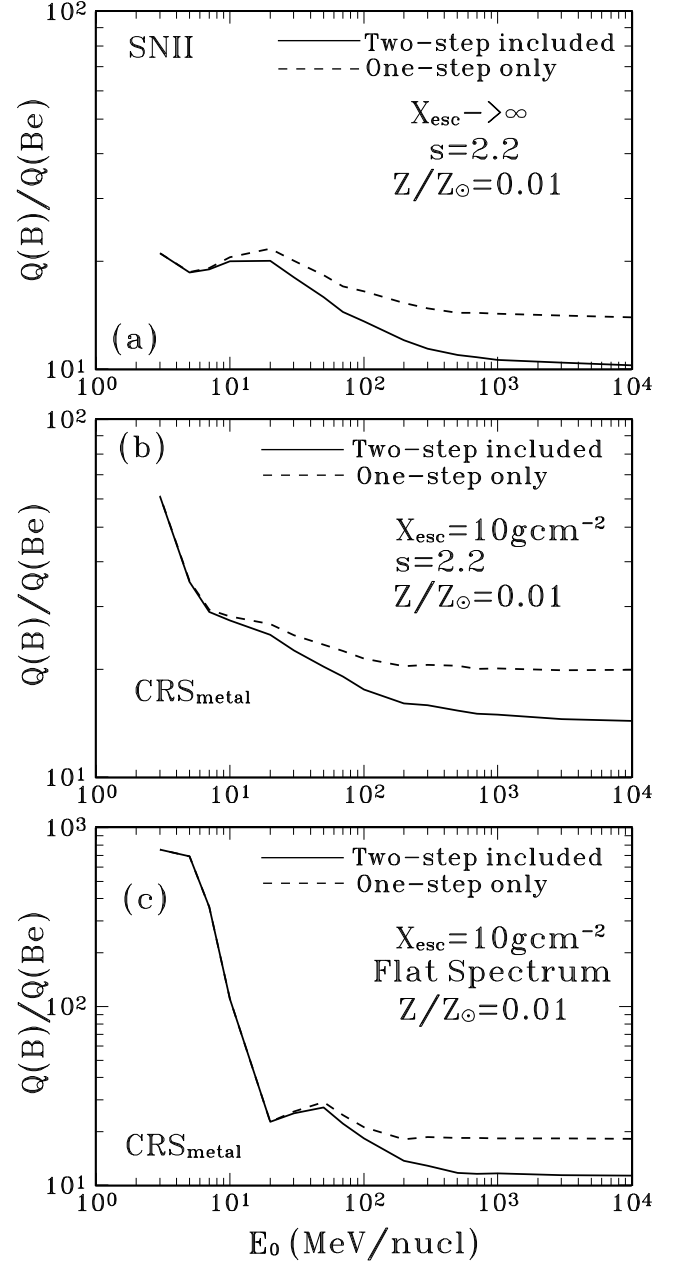


FIG. 4.—B/Be production ratios as a function of the characteristic energy  $E_0$  in eqs. (6) and (7) for a given ambient medium composition. The accelerated particle spectrum is from eq. (6) for (a) and (b) and from eq. (7) for (c). Panel (a) differs from panel (c) of Fig. 3 only in the choice of  $X_{\text{esc}}$ . Panels (b) and (c) are identical, except for the accelerated particle spectrum. The sharp cutoff at  $E_0$  in eq. (7) leads to the very large ratio at low energies in (c).

included. We see that  $Q(^{11}\text{B})/Q(^{10}\text{B})$  increases with decreasing  $E_0$ . For the strong shock spectrum, however,  $Q(^{11}\text{B})/Q(^{10}\text{B})$  is less than the meteoritic value of  $4.05 \pm 0.2$  (Chaussidon & Robert 1995) at all  $E_0$ , except at very low values for some of the compositions. For the flat spectrum,  $Q(^{11}\text{B})/Q(^{10}\text{B})$  equals the meteoritic value for  $\text{CRS}_{\text{metal}}$  in a narrow range of  $E_0$  from 30 to 50 MeV nucleon $^{-1}$  (Fig. 6c, dashed curve). This high value of  $Q(^{11}\text{B})/Q(^{10}\text{B})$  results from the contributions of  $^{12}\text{C}$ , for which the  $^{11}\text{B}$  cross section is higher and the corresponding threshold is lower than the cross section and threshold for  $^{10}\text{B}$  production. At low  $E_0$ ,

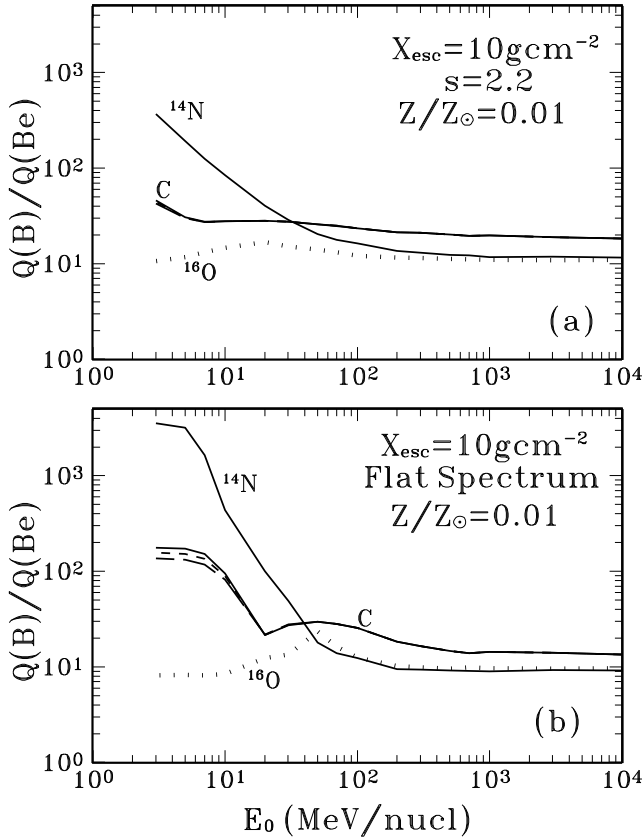


FIG. 5.—B/Be production ratios as functions of the characteristic energy  $E_0$  for a given ambient medium composition. Panels (a) and (b) are for the energy spectra given by eqs. (6) and (7), respectively. Pure C,  $^{14}\text{N}$ , and  $^{16}\text{O}$  are assumed for the accelerated particles. The effects of  $^{13}\text{C}$  can be seen for the C curve at low energies in (b):  $^{13}\text{C}/\text{C} = 0, 0.005, \text{ and } 0.01$  for the top, middle, and bottom branches, respectively.

$Q(^{11}\text{B})/Q(^{10}\text{B})$  is large mainly because of the contribution of  $^{14}\text{N}$ . This can be seen in Figure 7, where we show  $Q(^{11}\text{B})/Q(^{10}\text{B})$  resulting from accelerated particles consisting exclusively of either C (both  $^{12}\text{C}$  and  $^{13}\text{C}$ ),  $^{14}\text{N}$ , or  $^{16}\text{O}$ . The high value of  $Q(^{11}\text{B})/Q(^{10}\text{B})$  at low energies for  $^{14}\text{N}$  results from the low threshold reaction  $^{14}\text{N}(p, \alpha)^{11}\text{B}$  (Fig. 1). Even though  $Q(^{11}\text{B})/Q(^{10}\text{B})$  is suppressed at low energies by the presence of  $^{13}\text{C}$  (by the reaction  $^{13}\text{C}(p, \alpha)^{10}\text{B}$ ; Fig. 1),  $^{14}\text{N}$  has a larger contribution than  $^{13}\text{C}$  because of its larger relative abundance.

In Figure 8, we show the ratio of the Be production rate to the deposited power evaluated using equation (5). Figure 8a shows the dependence on  $Z/Z_\odot$ , while Figure 8b shows the dependence on  $E_0$ . We see (Fig. 8a) that  $Q(\text{Be})/\dot{W}$  is independent of  $Z/Z_\odot$  for the SNII<sub>metal</sub> and CRS<sub>metal</sub> compositions for which the Be is produced only in the inverse reactions.  $Q(\text{Be})/\dot{W}$  is nearly independent of  $Z/Z_\odot$  for the SNII and CRS compositions. However, for the SSz composition,  $Q(\text{Be})/\dot{W}$  increases linearly with metallicity from a very low value at  $Z/Z_\odot = 10^{-3}$ . As we shall see (§ 3.1), this very low initial  $Q(\text{Be})/\dot{W}$  rules out the SSz composition on the basis of energetics. Furthermore, as we shall also see (§ 3.1), the linear dependence of the production translates into a quadratic dependence of the inventory, which is inconsistent with observations. Concerning the dependence on  $E_0$ , we see (Fig. 8b) that  $Q(\text{Be})/\dot{W}$  is relatively constant for  $E_0$  greater than about 50 MeV nucleon $^{-1}$ . At lower

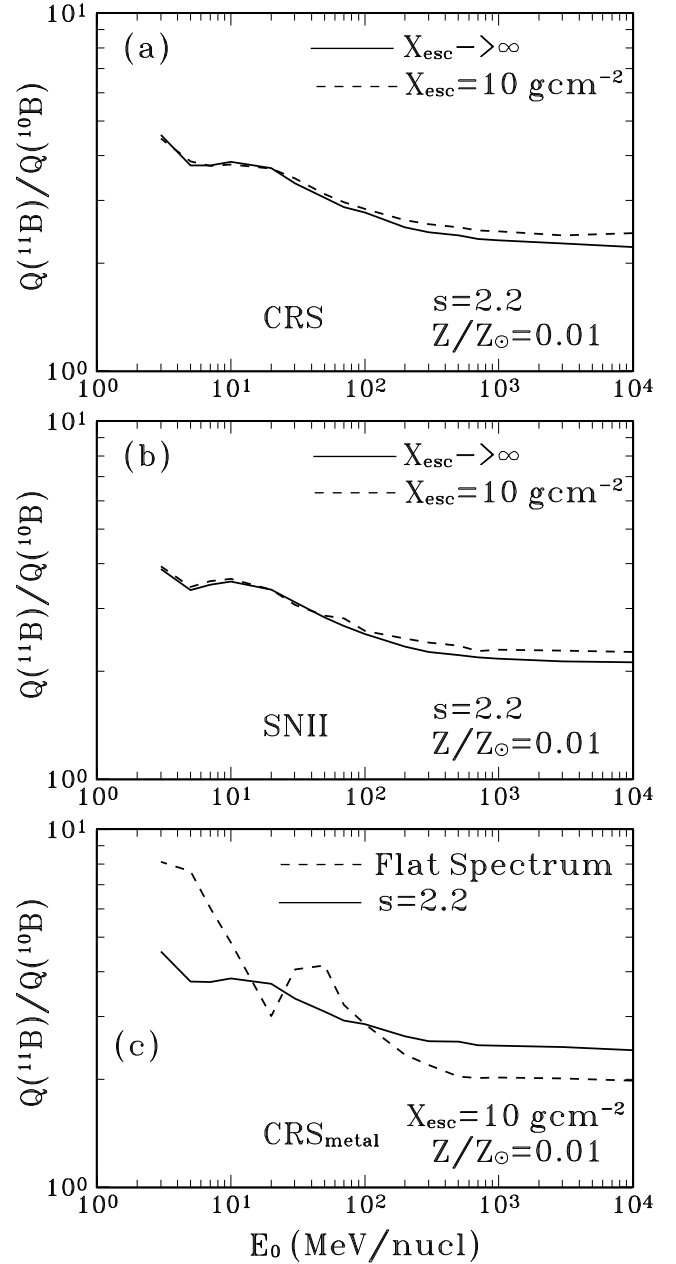


FIG. 6.— $^{11}\text{B}/^{10}\text{B}$  production ratios as a function of the characteristic energy  $E_0$  in eqs. (6) and (7) for a given ambient medium composition. The six curves shown in the three panels of this figure correspond to the same parameters as the six solid curves in Figs. 3 and 4. Curves with given values of  $s$  are for the spectrum of eq. (6); the flat spectrum is given in eq. (7).

values,  $Q(\text{Be})/\dot{W}$  decreases rapidly with decreasing  $E_0$ , a fact which, as we shall see, provides a strong argument against the production of the light elements predominantly by very low energy cosmic rays. The same effect can be seen in Figure 8c also, where we show  $Q(\text{Be})/\dot{W}$  as a function of  $E_0$  for various values of the spectral index  $s$ . As already mentioned, in calculating  $\dot{W}$ , we assumed a low-energy cutoff at 1 MeV nucleon $^{-1}$ . We see that even at the highest  $E_0$ ,  $Q(\text{Be})/\dot{W}$  becomes quite small when  $s = 7$ . As mentioned above, this value of  $s$  yields, in the nonrelativistic region, a power law in kinetic energy per nucleon with spectral index 4, which approximates the velocity distribution of the ejected mass of supernovae in their outer regions (Woosley,



Langer, & Weaver 1993). Thus, energetic arguments will allow us to rule out light-element production due to interactions caused by the bulk motion of the fast ejecta without subsequent acceleration.

In Figures 9a and 9b, we show the ratio of the  ${}^6\text{Li}$  production rate to the deposited power, again evaluated using equation (5). Figure 8a shows the dependence on  $Z/Z_\odot$ , while Figure 8b shows the dependence on  $E_0$ . We see that, similar to Be, the  ${}^6\text{Li}$  productions are independent of metallicity for the SNII<sub>metal</sub> and CRS<sub>metal</sub> compositions, and nearly independent for SNII and CRS. But unlike for Be, there is efficient  ${}^6\text{Li}$  production for the SSz composition also. This is due to the contributions of the  $\alpha$ - $\alpha$  reactions that allow cosmic rays with the SSz composition to produce significant amounts of  ${}^6\text{Li}$  in the early Galaxy. Figure 9c shows the  ${}^7\text{Li}/{}^6\text{Li}$  production ratio for selected compositions and accelerated particle energy spectra. We shall use these calculations in § 3.3 for the evolution of Li. The Li isotopic ratio is essentially the same for all relevant cases, very nearly equal to 1.5. The uncertainty in the  $\alpha$ - $\alpha$  cross sections at high energies (§ 2.1) introduces a  $\sim 35\%$  uncertainty in the total  ${}^6\text{Li}$  production, but only for the SSz composition and  $E_0 = 10^4$  MeV nucleon $^{-1}$ . For the other compositions and smaller  $E_0$ , the uncertainty is much smaller. The corresponding uncertainty in the  ${}^7\text{Li}/{}^6\text{Li}$  production ratio is negligible.

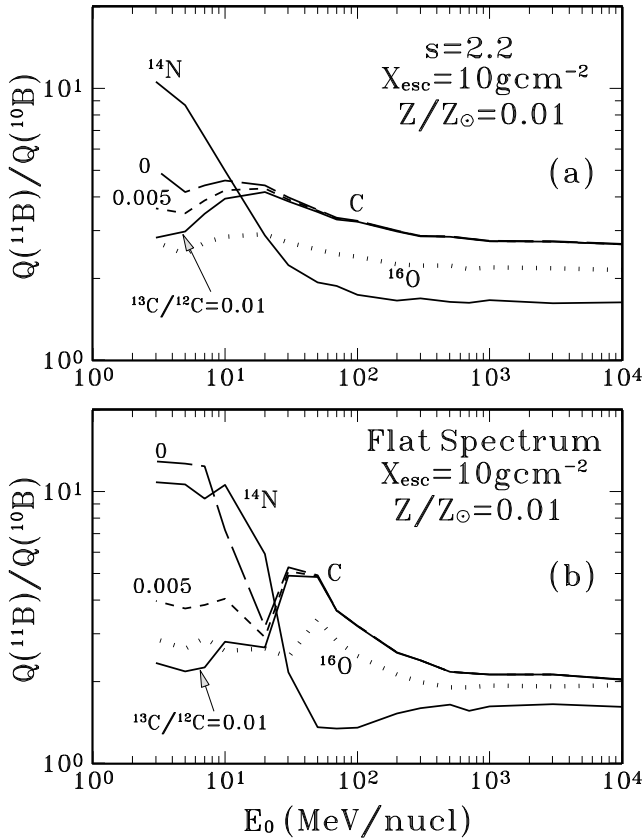


FIG. 7.— ${}^{11}\text{B}/{}^{10}\text{B}$  production ratios as functions of the characteristic energy  $E_0$  for a given ambient medium composition. Panels (a) and (b) are for the energy spectra given by eqs. (6) and (7), respectively. Pure C,  ${}^{14}\text{N}$ , and  ${}^{16}\text{O}$  are assumed for the accelerated particles. The effects of  ${}^{13}\text{C}$  can be seen for the C curve at low energies:  ${}^{13}\text{C}/\text{C} = 0, 0.005$ , and  $0.01$  for the top, middle, and bottom branches, respectively.

### 3. EVOLUTION

We limit our calculations of the Galactic evolution of Li, Be, and B to metallicities  $10^{-3} < Z/Z_\odot \equiv (\text{Fe}/\text{H})/(\text{Fe}/\text{H})_\odot < 0.1$ . This allows us to assume that the bulk of the Fe is produced by core collapse supernovae (SNII), with Type Ia supernovae not yet contributing significantly (Truran & Timmes 1994; Timmes, Woosley, & Weaver 1995). By averaging the calculated (Woosley & Weaver 1995)  ${}^{56}\text{Fe}$  yields per SNII over an IMF proportional to  $M^{-2.5}$  (e.g., Silk 1995), we obtain an  ${}^{56}\text{Fe}$  yield of approximately  $0.11 M_\odot/\text{SNII}$ , independent of metallicity. Next we rely on the observations that show that the abundance ratio Be/Fe is practically independent of metallicity over a broad range of  $Z/Z_\odot$ . Since the Be is produced by

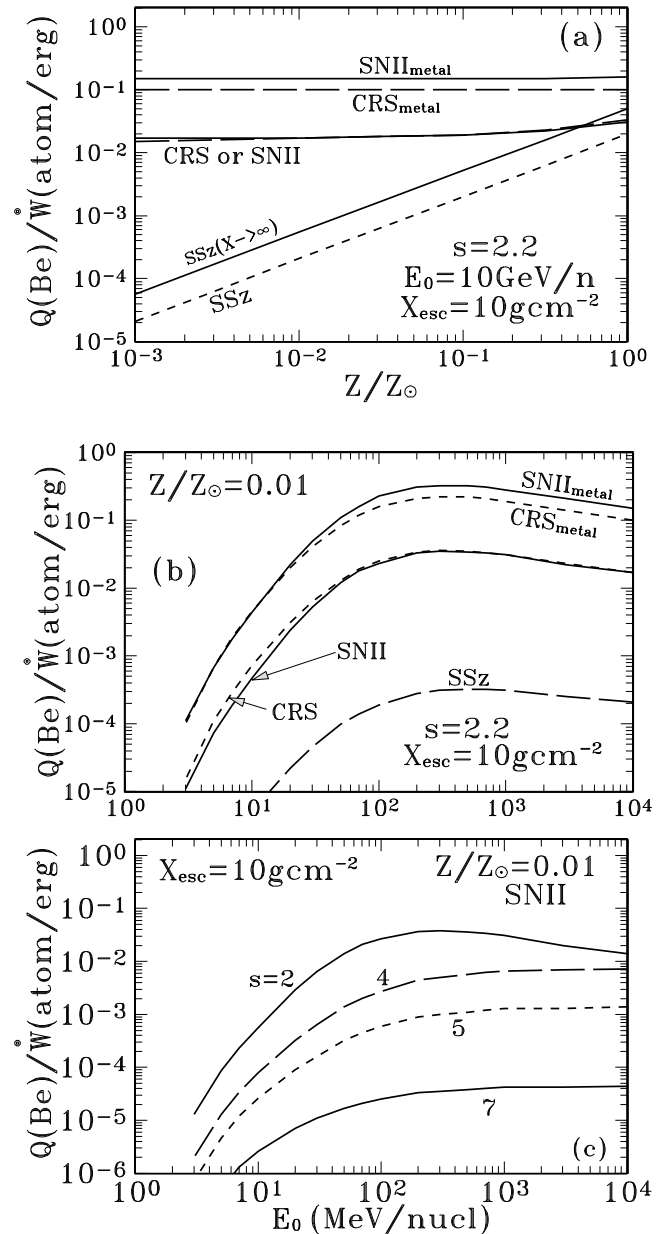


FIG. 8.—Ratios of Be production to the accompanying deposited power. The accelerated particle energy spectrum in all cases is from eq. (6). All curves are for the leaky box model,  $X_{\text{esc}} = 10 \text{ g cm}^{-2}$ , except the SSz ( $X_{\text{esc}} \rightarrow \infty$ ) case in (a), which is for a closed Galaxy.

cosmic rays, this constancy implies that the cosmic-ray acceleration is related to SNIIs also. We demonstrate quantitatively that because both the Fe yield per SNII and the abundance ratio Be/Fe are independent of metallicity, the removal rate of these elements from the Galactic inventory due to star formation is negligible compared with their production rate. This follows because the removal rates are proportional to the metallicity and very low at low metallicities, while the production rates are large and independent of metallicity. We thus can deal with the total Galactic Be and Fe inventories without having to consider the H inventory, which can vary, for example, because of continued infall. Furthermore, this approach allows us to simplify greatly the calculation of the Be inventory; in particular, we can obtain a straightforward estimate of the Be production

per SNII, which in turn leads directly to the energy in cosmic rays per SNII.

Concerning the evolution of B, in addition to production by cosmic rays, we also take into account  $^{11}\text{B}$  production by neutrinos in SNIIs (Woosley et al. 1990). A complication concerning this additional source was pointed out by Vangioni-Flam et al. (1996). In their model, the bulk of the Be in the early Galaxy is produced by low-energy cosmic rays related to just the SNIIs from very massive ( $> 60 M_{\odot}$ ) stellar progenitors. These massive stars have very short lifetimes, but if the early supernova rate was high enough, the lifetimes of the lowest mass stars ( $\sim 10 M_{\odot}$ ) that become SNIIs could be longer than the time required to produce the Galactic Fe inventory at metallicity of a few times  $10^{-3}$ . If this were the case, Fe and Be, as well as B and Be, would evolve quite differently because the B production by neutrinos is also due to SNIIs from all progenitors with masses greater than  $10 M_{\odot}$ . The constancy of Be/Fe, however, argues against such a possibility. Thus, either the acceleration and the Fe production are related to the same mass range of SNII progenitors or the supernova rate is low enough so that the time required to build up the Fe inventory to a metallicity of a few times  $10^{-3}$  is longer than the  $\sim 10^7$  yr lifetime of the lowest mass progenitors. We shall assume that one or both of these conditions are valid, so that we can ignore the difference in the lifetimes of the SNII progenitors of various masses and assume that the evolution of B is the same as that of Be.

Arguments similar to those advanced for Be and B also apply to the evolution of  $^6\text{Li}$ , as well as to the evolution of the  $^7\text{Li}$  resulting from cosmic rays and neutrinos in SNIIs. These arguments, however, do not apply to the total Li that is dominated by the very large initial contribution from big bang nucleosynthesis. In our treatment, we shall assume, based on the observations, that Li/H is constant in the range of metallicities that we consider. This will allow us to calculate the Li isotopic ratio, as well as the upper limits on the contribution to  $^7\text{Li}$  production by neutrino-induced nucleosynthesis.

### 3.1. Beryllium

The constancy of Be/Fe is equivalent to the frequently displayed linear dependence of Be/H as a function of Fe/H (e.g., Duncan et al. 1992, 1996; Cassé et al. 1995; Casuso & Beckman 1997; Lemoine et al. 1997). The linear relationship is valid particularly for  $Z/Z_{\odot} < 0.1$ , where the Be data can be fitted by

$$\frac{\text{Be}}{\text{H}} \simeq 5 \times 10^{-11} \frac{Z}{Z_{\odot}}, \quad (8)$$

which, with the solar  $\text{Fe}/\text{H} = 3.2 \times 10^{-5}$  (Grevesse, Noels, & Sauval 1996), implies that

$$\frac{\text{Be}}{\text{Fe}} \simeq 1.6 \times 10^{-6}. \quad (9)$$

We estimate that there is an error of about a factor of 2 in these ratios. Ignoring for the moment the removal due to star formation and the return of astrated material to the ISM, the evolution of the Be and Fe inventories (measured in number of atoms) can be written as

$$\text{Be}(t) = \int_0^t Q_{\text{Be}}(t') dt'; \quad \text{Fe}(t) = \int_0^t Q_{\text{Fe}}(t') dt', \quad (10)$$

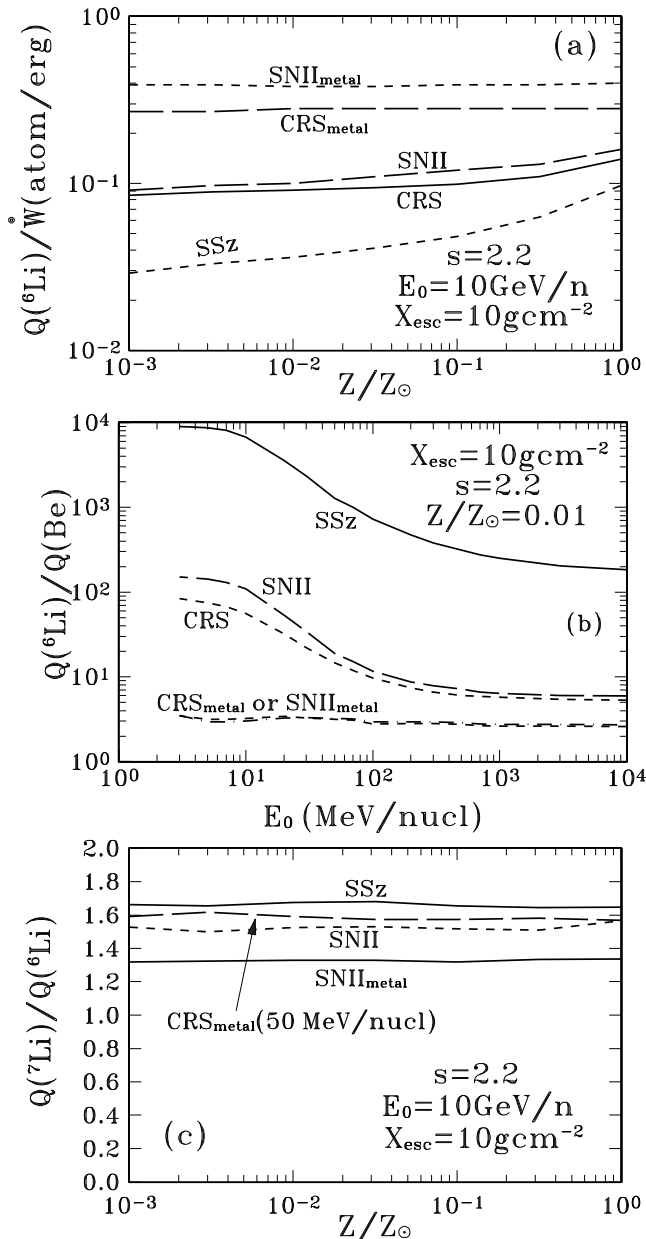


FIG. 9.—(a) Ratios of  $^6\text{Li}$  production to the accompanying deposited power. (b)  $^6\text{Li}/\text{Be}$  and (c)  $^7\text{Li}/^6\text{Li}$  production ratios. The accelerated particle energy spectrum in all cases is from eq. (6).  $E_0 = 10\text{ GeV nucleon}^{-1}$  for all cases in (c), except  $\text{CRS}_{\text{metal}}$ , for which  $E_0 = 50\text{ MeV nucleon}^{-1}$ .

where the  $Q$  are production rates (measured in atoms per second). Equation (10) also ignores the losses due to possible outflows from Galaxy. However, the infall of primordial matter has no effect on this equation. Using the integral for Fe, we can replace the time variable in the integral for Be by the iron inventory Fe. We obtain

$$\frac{\text{Be}}{\text{Fe}}(\text{Fe}) = \frac{1}{\text{Fe}} \int_0^{\text{Fe}} \frac{Q_{\text{Be}}(\text{Fe}')}{Q_{\text{Fe}}(\text{Fe}')} d(\text{Fe}'). \quad (11)$$

Since Be/Fe is observed to be constant as a function of  $Z/Z_\odot$ , it will also be constant as a function of Fe. Then the solution of equation (11) is  $Q_{\text{Be}}(\text{Fe})/Q_{\text{Fe}}(\text{Fe}) = \text{const}$ , and therefore also

$$\frac{Q_{\text{Be}}(Z/Z_\odot)}{Q_{\text{Fe}}(Z/Z_\odot)} = \text{const}, \quad (12)$$

where the constant is equal to the observed Be/Fe inventory ratio (eq. [9]). It should be noted that in the case of strong infall, the metallicity  $Z$  may not be a single-valued function of Fe, but we ignore this possibility here. Using the Fe yield per SNII of  $0.11 M_\odot$  given above, equation (12) implies that the average Be production associated with each SNII is  $3.8 \times 10^{48}$  atoms or  $2.8 \times 10^{-8} M_\odot$ , and that it is independent of  $Z/Z_\odot$ . As above, these values are uncertain within a factor of 2.

To see when the removal of Be and Fe can be ignored, let  $\dot{M}_{\text{SFR}}(t)$  be the removal rate of Galactic gas (mostly H) due to star formation (measured in mass/unit time). Assuming that all stars of mass greater than  $10 M_\odot$  form Type II supernovae, the SNII formation rate is

$$\dot{N}_{\text{SNII}} = \dot{M}_{\text{SFR}} \frac{\int_{10}^{m_{\text{max}}} \phi(m) dm}{\int_{0.1}^{m_{\text{max}}} m \phi(m) dm} \simeq 0.003 \frac{\dot{M}_{\text{SFR}}}{M_\odot}, \quad (13)$$

where  $\phi(m) \propto m^{-2.5}$  is the IMF given above (measured in number of stars per unit stellar mass) with a low-mass cutoff at  $0.1 M_\odot$ . As already mentioned, we ignore the very short time period between the formation of greater than  $10 M_\odot$  stars and the explosion of Type II supernovae. Using equation (13) and the Be and Fe productions per SNII of  $2.8 \times 10^{-8}$  and  $0.11 M_\odot$ , respectively, the Be and Fe production rates (measured in mass/unit time) are

$$P_{\text{Be}} \simeq 8.4 \times 10^{-11} \dot{M}_{\text{SFR}}; \quad P_{\text{Fe}} \simeq 3.3 \times 10^{-4} \dot{M}_{\text{SFR}}. \quad (14)$$

In terms of the same  $\dot{M}_{\text{SFR}}$ , the corresponding removal rates (also measured in mass/unit time) are

$$R_{\text{Be}} = 9(\text{Be}/\text{H}) \dot{M}_{\text{SFR}}(t); \quad R_{\text{Fe}} = 56(\text{Fe}/\text{H}) \dot{M}_{\text{SFR}}(t), \quad (15)$$

which, with  $\text{Be}/\text{H} = 5 \times 10^{-11} Z/Z_\odot$  and  $\text{Fe}/\text{H} = 3.2 \times 10^{-5} Z/Z_\odot$ , yield a production-to-removal ratio for both Be and Fe of

$$\frac{P}{R} \simeq \frac{0.2}{(Z/Z_\odot)}. \quad (16)$$

Thus, for  $Z/Z_\odot < 0.1$ ,  $P/R > 2$  (becoming  $\simeq 200$  for  $Z/Z_\odot = 10^{-3}$ ), allowing us to ignore the removal. As already mentioned, this important result is simply the consequence of the fact that, while the Be and Fe productions are independent of the metallicity of the ISM, their removal is proportional to the metallicity. The validity of this conclusion was confirmed by E. Vangioni-Flam (1996, private communication) using a light-element evolutionary code.

Parenthetically, we note that with a current rate of Galactic SNIIs of 3 per 100 yr (van den Bergh & Tammann 1991), equation (13) implies a star formation rate of  $\sim 10 M_\odot \text{ yr}^{-1}$ , which is not unreasonable.

Using the calculated  $Q_{\text{Be}}/\dot{W}$ , the Be yield per deposited power plotted in Figure 8a, we can define the Be production per SNII as  $W_{\text{SNII}}(Q_{\text{Be}}/\dot{W})$ , where  $W_{\text{SNII}}$  is the energy of an SNII going into the accelerated particles that produce the Be. If  $W_{\text{SNII}}$  is independent of  $Z/Z_\odot$  (a reasonable assumption), then all compositions except SSz produce an essentially constant Be yield per SNII (Fig. 8a), as required by the data.

We consider next the energy required to produce the Be. For the SNII and CRS compositions with  $E_0 = 10 \text{ GeV nucleon}^{-1}$ ,  $Q_{\text{Be}}/\dot{W} \simeq 0.017$  (Fig. 8a). Thus, the required Be production of  $3.8 \times 10^{48}$  atoms per SNII implies that  $W_{\text{SNII}} \simeq 2 \times 10^{50}$  ergs. This energy requirement is essentially equal to the energy per supernova that must be supplied to the Galactic cosmic rays (e.g., Lingenfelter 1992) assuming a supernova rate of 3 per 100 yr. Similarly, for the SNII<sub>metal</sub> and CRS<sub>metal</sub> compositions,  $Q_{\text{Be}}/\dot{W} \simeq 0.15$  and  $\simeq 0.1$ , respectively. The required energies per SNII for these purely metallic compositions are therefore  $2.5 \times 10^{49}$  and  $3.8 \times 10^{49}$  ergs, i.e., 11% and 17% of the total energy required for the CRS composition. This is essentially equal to the fraction of that total energy in the metallic component, since the Be is made predominantly by the accelerated metals interacting on ambient H and He and not by accelerated H and He in the low  $Z/Z_\odot$  ISM. For the SNII<sub>metal</sub> composition, this lower energy requirement compensates for the fact that the reverse shock, which we assume accelerates this composition, is expected to impart less energy to cosmic rays than the main supernova shock. In the case of the CRS<sub>metal</sub> composition, which could result from acceleration associated with SNIIs from just the most massive progenitors, the lower energy requirement compensates for the lower frequency of occurrence of supernovae from such progenitors. In particular, if the CRS<sub>metal</sub> composition results only from SNIIs from greater than  $60 M_\odot$  progenitors, with the IMF given above, the energy per event is approximately  $6 \times 10^{50}$  ergs. Thus, since for all four compositions, CRS, SNII, SNII<sub>metal</sub>, and CRS<sub>metal</sub>, reasonable energies per SNII are required to produce the Galactic Be inventory, any one of these scenarios could account for the Be data. In contrast, for the SSz composition at  $Z/Z_\odot = 10^{-3}$ , the energy requirement per SNII is  $6 \times 10^{52}$  ergs for  $X_{\text{esc}} \rightarrow \infty$  and  $2 \times 10^{53}$  ergs for  $X_{\text{esc}} = 10 \text{ g cm}^{-2}$ , which greatly exceed the total available mechanical energy of  $\sim 10^{51}$  ergs in the supernova ejecta. Even though these energetic requirements decrease with increasing metallicity, they are obviously excessive and thus provide very strong model-independent arguments against Be production by cosmic rays accelerated out of the ISM at low metallicities.

Considering the dependence of the Be production on the cosmic-ray spectrum (Fig. 8b), and assuming that the available energy per SNII is no more than  $3 \times 10^{50}$  ergs for the CRS and SNII compositions, which would require an efficiency of  $\leq 30\%$  for the conversion of mechanical energy of the ejecta into accelerated particle energy, we conclude that the spectral parameter  $E_0$  must be larger than about 50 MeV nucleon $^{-1}$ . For the SNII<sub>metal</sub> composition, we only take  $3 \times 10^{49}$  ergs because of the lower expected energy in the reverse shock. We take the same energy per average SNII for the CRS<sub>metal</sub> composition to allow for the lower

frequency of the very massive progenitors. Thus, in these cases as well,  $E_0$  must be greater than 50 MeV nucleon<sup>-1</sup>. The production of the Galactic Be therefore cannot be due to cosmic rays with very low cutoff energies or very steep energy spectra.

Fields et al. (1996) suggested that significant light-element production could be due to the interactions of the ejecta of supernovae whose bulk velocities in the outer regions correspond to particle energies above the thresholds for nuclear reactions and extend to about 10 MeV nucleon<sup>-1</sup>. As mentioned above (§ 2.2), the velocity distribution in the ejecta corresponds to a power-law spectrum in kinetic energy per nucleon with index  $\sim 4$ . For our assumed spectra (eq. [6]), the corresponding parameters are  $s = 7$  and  $E_0 = 10$  MeV nucleon<sup>-1</sup>. From Figure 8c, it then follows that  $Q/\dot{W} \simeq 3 \times 10^{-6}$ . Assuming that the supernova ejecta contain  $10^{51}$  ergs, the required Be production of  $3.8 \times 10^{48}$  atoms per SNII implies that only 0.1% of the Galactic Be can be produced by supernova ejecta without additional acceleration. A somewhat similar conclusion was obtained by Vangioni-Flam et al. (1996).

Even though the Be data require the existence in the early Galaxy of cosmic rays rich in metals (CRS, SNII, CRS<sub>metal</sub>, or SNII<sub>metal</sub>), this does not rule out the simultaneous existence of cosmic rays accelerated out of the ISM (SSz), as long as the energy in such cosmic rays is not excessively large, so that the constancy of Be/Fe is maintained. We thus calculate the Galactic Be inventory by combining the contributions of a metal-rich cosmic-ray component with that of a component with the SSz composition. To limit the number of possible combinations, and without loss of generality, we take the metal-rich component to be either SNII<sub>metal</sub>, SNII, or CRS<sub>metal</sub>, with  $E_0 = 10$  GeV nucleon<sup>-1</sup> for SNII<sub>metal</sub> and SNII, and  $E_0 = 50$  MeV nucleon<sup>-1</sup> for CRS<sub>metal</sub>. For the metal-poor SSz component, we also take  $E_0 = 10$  GeV nucleon<sup>-1</sup>. The production rates for the resultant three models are given in Table 3, where  $A \equiv \text{Be/Fe}$  (eq. [9]) and  $\xi$  is the ratio between the energies supplied to the metal-poor and metal-rich cosmic-ray components. We normalize all the productions to the observed constant Be/Fe inventory ratio. This, together with the fact that  $A$  is independent of  $Z/Z_\odot$ , ensures that the metal-rich component yields the observed Be/Fe as long as  $\xi$  is low

enough. For all cases, we use the spectrum of equation (6) and assume  $X_{\text{esc}} = 10 \text{ g cm}^{-2}$ . The expressions for the <sup>6</sup>Li and <sup>7</sup>Li productions, as well as for the Be production for the SSz composition, are obtained from Figures 8 and 9. The implications of the Li productions, including the neutrino-induced <sup>7</sup>Li production, are considered in § 3.3.

By making the simplifying assumption that the total Galactic H inventory is independent of metallicity (an assumption that was so far unnecessary), and by replacing the Fe variable with  $Z/Z_\odot$  in equation (11), we obtain

$$\frac{\text{Be}}{\text{H}} = Z_\odot \int_0^{Z/Z_\odot} \frac{Q_{\text{Be}}(\eta)}{Q_{\text{Fe}}} d\eta = AZ_\odot \times \left[ \frac{Z}{Z_\odot} + (0.13 \text{ or } 1.2 \text{ or } 0.24) \frac{\xi}{2} \left( \frac{Z}{Z_\odot} \right)^2 \right], \quad (17)$$

where we evaluated the integral by using the productions given in Table 3 for Be. The requirement that the quadratic term up to  $Z/Z_\odot < 0.1$  be negligible for Be (e.g., less than 20% of the linear term) sets upper limits,  $\xi < 30$ ,  $\xi < 3$ , and  $\xi < 15$ , for the three models considered in Table 3. As the required energies in metal-rich cosmic rays per SNII for the three models are  $2.5 \times 10^{49}$ ,  $2.2 \times 10^{50}$ , and  $4.2 \times 10^{49}$  ergs, these upper limits allow energies in the metal-poor component of about  $7 \times 10^{50}$  ergs, independent of the model.

### 3.2. Boron

Unlike Be, in addition to the cosmic-ray production, B is also produced by neutrinos in SNIIs. As for <sup>56</sup>Fe, we have averaged the calculated (Woosley & Weaver 1995)  $\nu$ -produced <sup>11</sup>B yields per SNII and found only small variations with  $Z/Z_\odot$ . For the IMF proportional to  $m^{-2.5}$ , we obtain an essentially constant <sup>11</sup>B yield of about  $6.5 \times 10^{-7} M_\odot$  per SNII. We define the ratio of the neutrino-produced mass of <sup>11</sup>B to the mass of <sup>56</sup>Fe per SNII,

$$R(11_\nu, 56) = \frac{M_{11}}{M_{56}}, \quad (18)$$

so that a nominal value of  $R \sim 6 \times 10^{-6}$  is expected from  $\nu$ -production calculations and an IMF-averaged <sup>56</sup>Fe production of  $0.11 M_\odot$  per SNII.

TABLE 3  
Be AND Li PRODUCTION RATIOS (BY NUMBER),  $Q/Q_{\text{Fe}}$

Element and Isotopes	Metal-Rich Cosmic-Ray Composition	Metal-Poor Cosmic-Ray Composition	$\nu$
Model 1: SNII <sub>metal</sub> ( $E_0 = 10$ GeV nucleon <sup>-1</sup> ), SSz ( $E_0 = 10$ GeV nucleon <sup>-1</sup> )			
Be .....	$A$	$0.13 Z/Z_\odot A \xi$	...
<sup>6</sup> Li .....	$2.6A$	$0.26A \xi$	...
<sup>7</sup> Li .....	$3.5A$	$0.42A \xi$	(56/7) $R(7_\nu, 56)$
Model 2: SNII ( $E_0 = 10$ GeV nucleon <sup>-1</sup> ), SSz ( $E_0 = 10$ GeV nucleon <sup>-1</sup> )			
Be .....	$A$	$1.2A \xi$	...
<sup>6</sup> Li .....	$6.9A$	$2.5A \xi$	...
<sup>7</sup> Li .....	$10.0A$	$4.0A \xi$	(56/7) $R(7_\nu, 56)$
Model 3: CRS <sub>metal</sub> ( $E_0 = 50$ MeV nucleon <sup>-1</sup> ), SSz ( $E_0 = 10$ GeV nucleon <sup>-1</sup> )			
Be .....	$A$	$0.24 Z/Z_\odot A \xi$	...
<sup>6</sup> Li .....	$3.4A$	$0.47A \xi$	...
<sup>7</sup> Li .....	$5.4A$	$0.75A \xi$	(56/7) $R(7_\nu, 56)$

NOTE.— $A \equiv \text{Be/Fe}$  (eq. [9]), and  $\xi$  is the ratio between the energies supplied to the metal-poor and metal-rich cosmic-ray components. We normalize all the productions to the observed constant Be/Fe inventory ratio.

Like Be, the B/Fe ratio is also observed to be nearly independent of metallicity (Duncan et al. 1992, 1996). Therefore, an equation similar to equation (11) can be written for B as well. Furthermore, since the B/Be production ratio is independent of metallicity (Fig. 2), as is the B yield per SNII due to neutrinos, the B/Be inventory ratio should equal the production ratio  $Q_{\text{Be}}/Q_{\text{B}}$ . Thus, combining the cosmic-ray and neutrino contributions, we obtain

$$\frac{B}{\text{Be}} = \left[ \frac{Q(\text{B})}{Q(\text{Be})} \right]_{\text{cr}} + \frac{[Q(^{11}\text{B})]_{\nu}}{[Q(\text{Be})]_{\text{cr}}} \quad (19)$$

Using equation (18), we obtain

$$\frac{B}{\text{Be}} \simeq \left[ \frac{Q(\text{B})}{Q(\text{Be})} \right]_{\text{cr}} + \frac{56}{11} \frac{R(11_{\nu}, 56)}{(\text{Be}/\text{Fe})}, \quad (20)$$

where Be/Fe is given by equation (9).

Combining the cosmic-ray and neutrino-induced B productions, the following relationship between production ratios can be derived:

$$\frac{Q(\text{B})}{Q(\text{Be})} = \left[ \frac{Q(\text{B})}{Q(\text{Be})} \right]_{\text{cr}} \frac{[Q(^{11}\text{B})/Q(^{10}\text{B})] + 1}{[Q(^{11}\text{B})/Q(^{10}\text{B})]_{\text{cr}} + 1}, \quad (21)$$

where  $Q(^{11}\text{B})/Q(^{10}\text{B})$  and  $Q(\text{B})/Q(\text{Be})$  include both the cosmic-ray and neutrino productions. As established above, the B/Be production ratio can be replaced by the corresponding inventory ratio. Similarly, the  $^{11}\text{B}/^{10}\text{B}$  production ratio by cosmic rays is independent of metallicity, and the  $^{11}\text{B}$  production per SNII by neutrinos is also metallicity independent. Thus, we can replace the B/Be and  $^{11}\text{B}/^{10}\text{B}$  production ratios by the corresponding inventory ratios. We obtain

$$\frac{B}{\text{Be}} = \left[ \frac{Q(\text{B})}{Q(\text{Be})} \right]_{\text{cr}} \frac{(^{11}\text{B}/^{10}\text{B}) + 1}{[Q(^{11}\text{B})/Q(^{10}\text{B})]_{\text{cr}} + 1}. \quad (22)$$

Since  $^{11}\text{B}/^{10}\text{B}$  has not been measured yet in the early Galaxy, we treat it as a free parameter. By substituting equation (22) into equation (20) and by using  $[Q(\text{B})/Q(\text{Be})]_{\text{cr}}$  and  $[Q(^{11}\text{B})/Q(^{10}\text{B})]_{\text{cr}}$  plotted in Figures 3, 4, and 6, we solve for  $R(11_{\nu}, 56)/(\text{Be}/\text{Fe})$ , the ratio of the  $\nu$ -produced  $^{11}\text{B}$  to Fe per SNII normalized to the number ratio Be/Fe given by equation (9). The results are shown in Figures 10 and 11 for the various cosmic-ray models and various values of the B inventory isotopic ratio,  $^{11}\text{B}/^{10}\text{B}$ . The corresponding elemental inventory ratio, B/Be, is plotted in Figures 12 and 13 for the same cosmic-ray models and the same assumed values for  $^{11}\text{B}/^{10}\text{B}$ . We see that for  $^{11}\text{B}/^{10}\text{B} = 2$ ,  $R(11_{\nu}, 56) = 0$ , and thus no neutrino contribution is needed. This is obvious since cosmic-ray spallation will always produce a B isotopic ratio greater than 2. However, larger values of  $^{11}\text{B}/^{10}\text{B}$  do require a  $\nu$  contribution to  $^{11}\text{B}$  production, except for some models at very low values of  $E_0$  (Fig. 11b for  $^{11}\text{B}/^{10}\text{B} = 3$  and Fig. 11c for all  $^{11}\text{B}/^{10}\text{B}$ ). In addition, no neutrino contribution is required for  $^{11}\text{B}/^{10}\text{B} = 4$  in the narrow range  $30 < E_0 < 50$  MeV nucleon $^{-1}$  for the CRS<sub>metal</sub> composition with the flat spectrum (Fig. 11c). Despite the fact that at low  $E_0$ , the cosmic-ray-produced B isotopic ratio is quite large, we see that for some of the models, especially for the CRS<sub>metal</sub> composition with the flat spectrum (Fig. 11c), a very large  $R$  is required to produce the B inventory ratio of 7. This is caused by the fact that at low  $E_0$ , the B/Be production by cosmic rays is very high. Consequently, the required Be yield per SNII implies a very

large B yield, which in turn requires a very large mass of  $\nu$ -produced  $^{11}\text{B}$  per SNII to account for the assumed B isotopic ratio.

Even though  $^{11}\text{B}/^{10}\text{B}$  has not been measured for low-metallicity stars, it probably should not be less than the solar system value of  $4.05 \pm 0.2$  (Chaussidon & Robert 1995), because at higher metallicities, when Type Ia supernovae start making an important contribution to the Fe abundance, cosmic-ray acceleration is not necessarily accompanied by  $^{11}\text{B}$  production by neutrinos as is the case

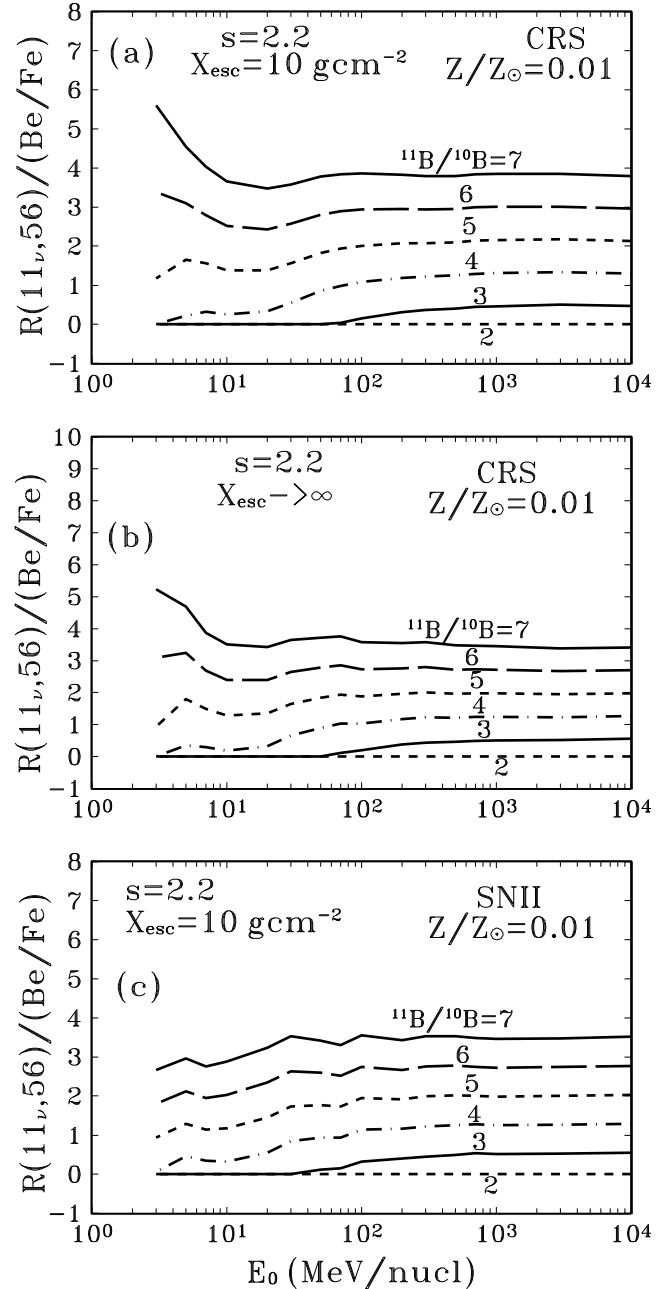


FIG. 10.—The ratio of the  $\nu$ -produced  $^{11}\text{B}$  mass to the  $^{56}\text{Fe}$  mass per SNII required to yield a given  $^{11}\text{B}/^{10}\text{B}$  ratio for various cosmic-ray models as a function of  $E_0$  in eq. (6). The ratio of the  $\nu$ -produced mass to the  $^{56}\text{Fe}$  mass is normalized to Be/Fe given in eq. (9). The range of plotted values can be compared with the nominal expected value of for  $R(11_{\nu}, 56)/(\text{Be}/\text{Fe})$  of  $\sim 3.7$  from eqs. (9) and (18).

when core collapse supernovae predominate. Thus, except for the  $\text{CRS}_{\text{metal}}$  composition and the rather artificial flat spectrum (eq. [7]) with  $30 < E_0 < 50$ , this constraint on  $^{11}\text{B}/^{10}\text{B}$  implies that  $^{11}\text{B}$  production via  $\nu$  spallation in SNIIs is essentially always required. We exclude  $E_0$  less than 10 MeV nucleon $^{-1}$  because such values are energetically extremely unfavorable (§ 3.1). If we limit  $E_0$  to values greater than 50 MeV nucleon $^{-1}$  (§ 3.1), then the requirement that  $^{11}\text{B}/^{10}\text{B} > 4$  implies that  $R(11\nu, 56)/(\text{Be}/\text{Fe}) > 1$  (Figs. 10a–11c).

The observed B/Be in low-metallicity stars is quite uncertain, mainly because of non-LTE effects (Edvardsson et al. 1994; Fields, Olive, & Schramm 1995; Kiselman & Carlsson 1996). One of the best observed stars is HD 140283, for which Fields et al. (1995) give  $\text{B}/\text{Be} = 6 \pm 2$  assuming LTE

and  $17 < \text{B}/\text{Be} < 25$  with non-LTE corrections included. As can be seen from Figures 12 and 13, if  $^{11}\text{B}/^{10}\text{B} > 4$ , B/Be cannot be lower than about 16, a value that is achieved for  $E_0 = 10$  GeV, the SNIi composition, and  $X_{\text{esc}} \rightarrow \infty$  (Fig. 13a). Thus, without the inclusion of non-LTE corrections, B/Be is inconsistent with  $^{11}\text{B}/^{10}\text{B} > 4$ , implying that the non-LTE corrections are necessary, provided of course that  $^{11}\text{B}/^{10}\text{B}$  in low-metallicity stars is at least as high as in the solar system. Concerning the upper end of the B/Be range, Edvardsson et al. (1994) limit B/Be to values less than about 34. Considering Figures 10–13, this implies that  $^{11}\text{B}/^{10}\text{B} < 7$  (except in some cases where it could be slightly higher, e.g., Fig. 13a for  $E_0 > 20$  MeV nucleon $^{-1}$ ). Limiting ourselves again to  $E_0 > 50$  MeV nucleon $^{-1}$ , this implies that  $R(11\nu, 56)/(\text{Be}/\text{Fe}) < 4$ . Combining this limit with that

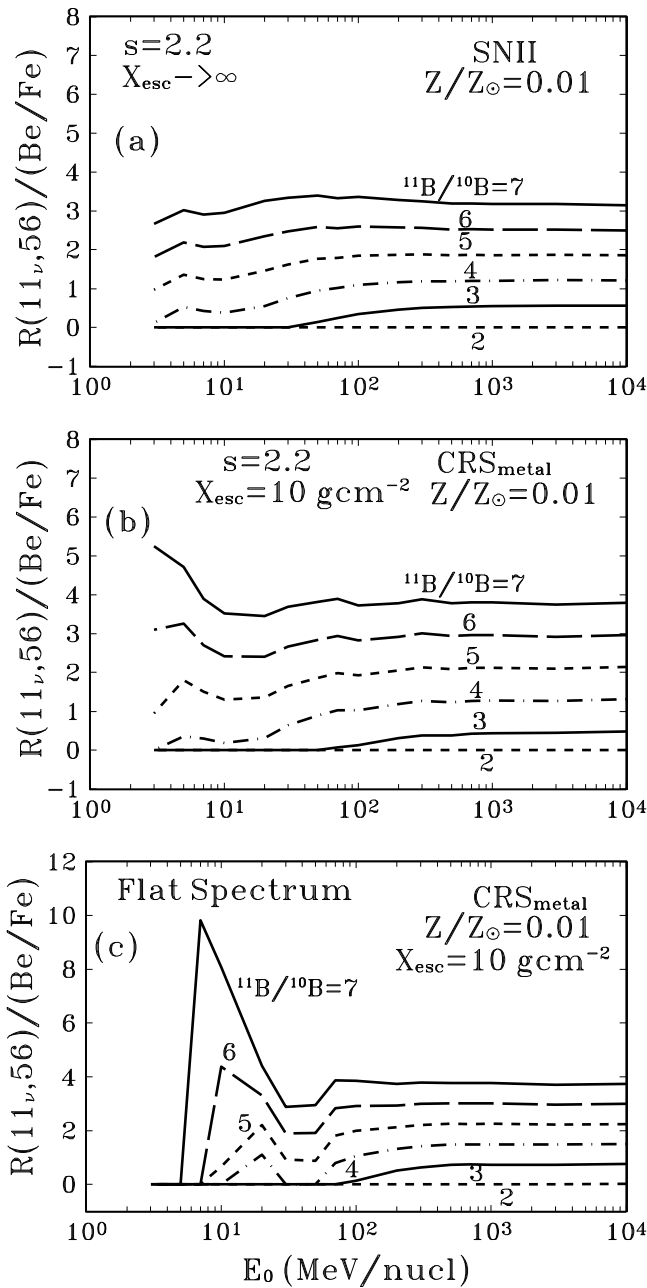


FIG. 11.—Same as Fig. 10, but for different cosmic-ray models

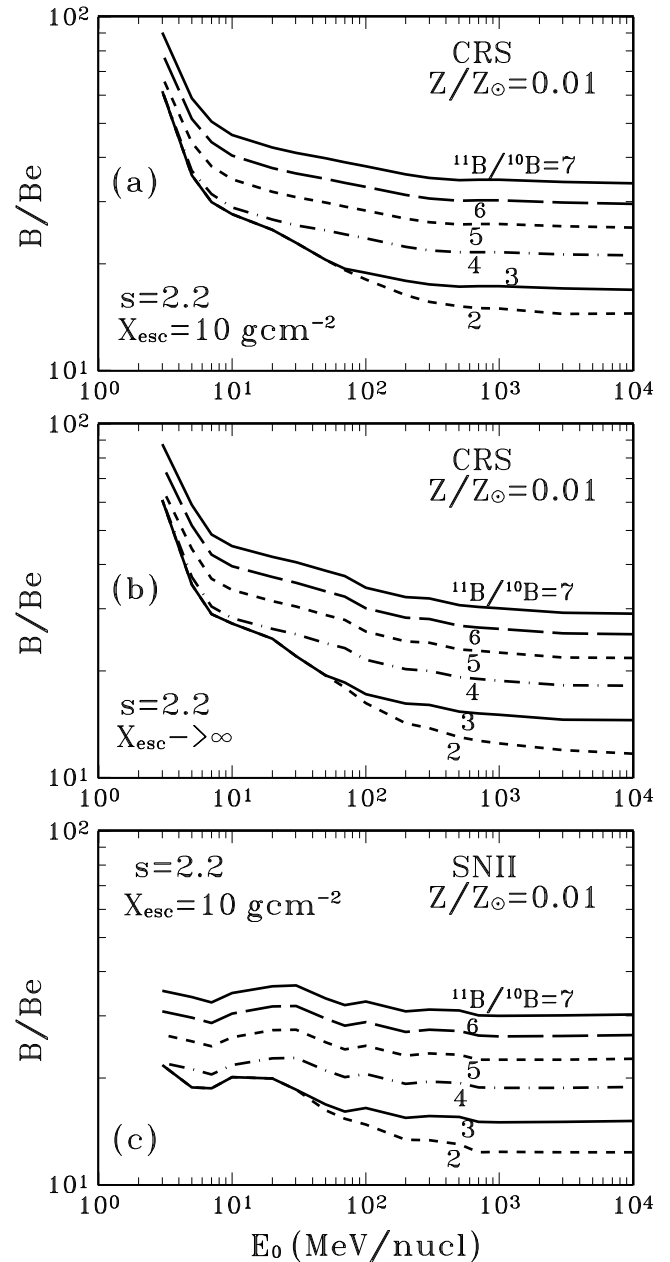


FIG. 12.—B/Be calculated from eq. (22) for the same cosmic-ray models as used in Fig. 10. This figure shows the implied B/Be ratio for a particular choice of  $^{11}\text{B}/^{10}\text{B}$  for the given cosmic-ray model.

obtained from the lower limit on  $^{11}\text{B}/^{10}\text{B}$ , we obtain

$$1 < \frac{R(11, 56)}{\text{Be/Fe}} < 4. \quad (23)$$

Using equation (9) and the SNII-produced Fe mass of  $0.11 M_\odot$ , we find that the neutrino-produced  $^{11}\text{B}$  mass  $M_{11}$  lies in the range

$$1.8 \times 10^{-7} M_\odot < M_{11} < 7.0 \times 10^{-7} M_\odot. \quad (24)$$

Given the uncertainty of a factor of 2 in Be/Fe, this range is not inconsistent with the nominal Woosley & Weaver (1995) yield of  $6.5 \times 10^{-7} M_\odot$  given above.

### 3.3. Lithium

There are at least three sources of Li in the early Galaxy, nucleosynthesis in the big bang (e.g., Reeves 1994), cosmic-

ray interactions, and neutrino-induced nucleosynthesis in SNIIs (Woosley & Weaver 1995). Unlike Be and B, however, cosmic rays produce Li not only via the spallation of metals but also in  $\alpha$ - $\alpha$  reactions. From Figure 9a, we see that, similar to Be (Fig. 8a), the  $^6\text{Li}$  productions are independent of metallicity for the SNII<sub>metal</sub> and CRS<sub>metal</sub> compositions, and nearly independent for SNII and CRS. We also see that unlike Be and B, the production of  $^6\text{Li}$  is very efficient with the SSz composition because the  $\alpha$ - $\alpha$  reactions allow very low metallicity cosmic rays to produce significant amounts of  $^6\text{Li}$  in the early Galaxy.

The best measurement of the Li isotopic ratio,  $^6\text{Li}/\text{Li}$ , in the early Galaxy that appears to be free of destruction effects is from the star HD 84937 (Smith, Lambert, & Nissen 1993; Hobbs & Thornburn 1994). We plot this ratio in Figure 14, where we took the error bars from the summary of Lemoine et al. (1997). This isotopic ratio can be written as

$$\frac{^6\text{Li}}{\text{Li}} = \frac{^6\text{Li/Be}}{\text{Li/H}} \frac{\text{Be}}{\text{H}}, \quad (25)$$

where all quantities denote Galactic inventories. We now evaluate equation (25) for the three models of Table 3. The  $^6\text{Li}$  production for the SNII<sub>metal</sub> (10 GeV nucleon $^{-1}$ ) and CRS<sub>metal</sub> (50 MeV nucleon $^{-1}$ ) cases is independent of metallicity (Fig. 9a and calculations not shown). We also have approximated the SNII (10 GeV nucleon $^{-1}$ ) and SSz (10 GeV nucleon $^{-1}$ )  $^6\text{Li}$  productions by constants in Table 3, because the  $^6\text{Li}$  productions for these cases are slowly varying functions of metallicity (Fig. 9a). Then, by excluding the SSz composition for Be because of its incompatibility with Be evolution (§ 3.1), we find that the  $^6\text{Li}/\text{Be}$  production ratio is independent of metallicity for all three models. Thus, we can replace the  $^6\text{Li}/\text{Be}$  inventory ratio in equation (25) by a production ratio,

$$\frac{^6\text{Li}}{\text{Li}} = \frac{Q(^6\text{Li})/Q(\text{Be})}{\text{Li/H}} \frac{\text{Be}}{\text{H}}. \quad (26)$$

The dashed lines in Figure 14 were obtained from equation (26) using the  $^6\text{Li}$  and Be productions given in Table 3 for the assumed three models, Be/H from equation (8), and Li/H =  $1.7 \times 10^{-10}$  (Spite plateau; e.g., Lemoine et al. 1997). We see that with  $\xi = 0$  (i.e., negligible contribution from the metal-poor component), we underproduce the  $^6\text{Li}$ . But the addition of the metal-poor component with a  $\xi$  near the upper limit allowed by the Be data could lead to sufficient  $^6\text{Li}$  production. Other acceptable models not considered in Table 3, for example, SNII (50 MeV nucleon $^{-1}$ ) for the metal-rich component (Fig. 9b) with  $\xi = 0$ , could lead to even higher  $^6\text{Li}/\text{Li}$ .

However, if the  $^6\text{Li}/\text{Be}$  production ratio is independent of metallicity,  $^6\text{Li}/\text{Li}$  at low metallicities cannot be arbitrarily large because its linear growth (eq. [26]) will conflict with the measured Li/H (Spite plateau) at metallicity near 0.1. The  $^6\text{Li}$  production by cosmic rays is accompanied by the production of  $^7\text{Li}$  with a production ratio independent of metallicity (Fig. 9c). In addition,  $^7\text{Li}$  could be produced in SNIIs by  $\nu$ -induced  $^3\text{He}$ - $^4\text{He}$  fusion. We have IMF-averaged the calculated (Woosley & Weaver 1995)  $\nu$ -induced  $^7\text{Li}$  productions per SNII and again found only small variations with  $Z/Z_\odot$ . Thus, the  $^7\text{Li}/\text{Be}$  production ratio due to this process is also independent of metallicity. For the IMF proportional to  $m^{-2.5}$ , we obtain a  $^7\text{Li}$  yield of about  $4 \times 10^{-7} M_\odot$  per SNII. As for  $^{11}\text{B}$ , we define the

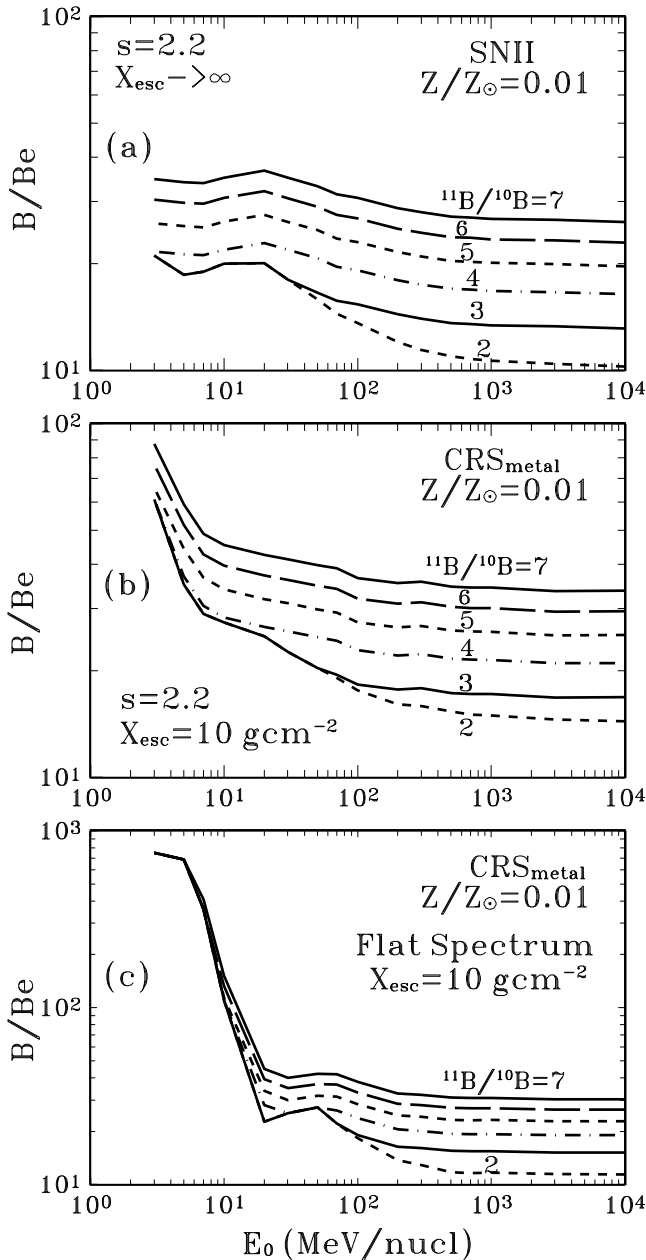


FIG. 13.—Same as Fig. 12, except that the correspondence is with Fig. 11.

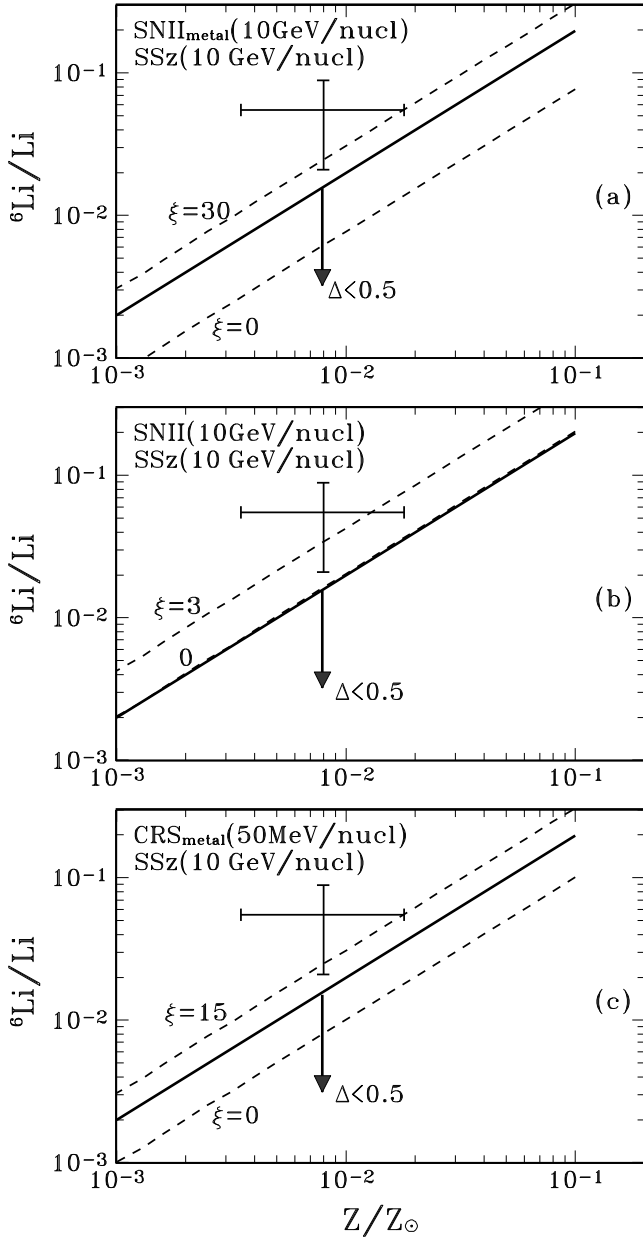


FIG. 14.—Observed  ${}^6\text{Li}/\text{Li}$  (Smith et al. 1993; Hobbs & Thornburn 1994; Lemoine et al. 1997). The dashed lines are from eq. (26), with  $Q({}^6\text{Li})/Q(\text{Be})$  obtained from Table 3 by combining the metal-poor component (SSz) with a metal-rich component. The nonzero values of  $\xi$ , the ratio of the energies in the metal-poor to metal-rich cosmic-ray components, correspond to upper limits set by the requirement of a constant  $\text{Be}/\text{Fe}$ . The solid lines are from eq. (29), with  $Q_v = 0$ ,  $Q_{\text{cr}}(\text{Li})/Q({}^6\text{Li}) \simeq 2.5$ , and  $\Delta = 0.5$ .

ratio of the  $\nu$ -produced  ${}^7\text{Li}$  mass to the mass of  ${}^{56}\text{Fe}$  per SNII,

$$R(7_\nu, 56) = \frac{M_7}{M_{56}}, \quad (27)$$

so that a nominal value of  $R(7_\nu, 56) \sim 3.6 \times 10^{-6}$  is expected from  $\nu$ -production calculations and an IMF-averaged  ${}^{56}\text{Fe}$  production of  $0.11 M_\odot$  per SNII. This  $\nu$ -produced  ${}^7\text{Li}$  is also shown in Table 3.

For consistency with the constant  $\text{Li}/\text{H}$  for  $Z/Z_\odot < 0.1$  (Spite plateau), the additional Li inventory due to cosmic-

ray and neutrino production must satisfy

$$\left(\frac{\text{Li}}{\text{H}}\right)_{\text{cr}, \nu} = \left\{ \left[ \frac{Q(\text{Li})}{Q(\text{Be})} \right]_{\text{cr}} + \left[ \frac{Q(\text{Li})}{Q(\text{Be})} \right]_{\nu} \right\} \frac{\text{Be}}{\text{H}} < \Delta \frac{\text{Li}}{\text{H}}, \quad (28)$$

where  $\text{Be}/\text{H}$  is evaluated at  $Z/Z_\odot = 0.1$ , and the multiplicative factor  $\Delta$  takes into account the spread in the observed values of  $\text{Li}/\text{H}$ . By combining equations (26) and (28), we obtain

$$\frac{{}^6\text{Li}}{\text{Li}} < 10\Delta \frac{Q({}^6\text{Li})}{Q_{\text{cr}}(\text{Li}) + Q_\nu({}^7\text{Li})} \left( \frac{Z}{Z_\odot} \right). \quad (29)$$

The upper limits on  ${}^6\text{Li}/\text{Li}$ , shown by the solid lines in Figure 14, were obtained from equation (29) by taking  $\Delta = 0.5$ , setting the  $\nu$ -produced Li to zero, and using  $Q_{\text{cr}}(\text{Li})/Q({}^6\text{Li}) \simeq 2.5$  (Fig. 9c). We see that the upper limit set by the constant  $\text{Li}/\text{H}$  on the cosmic-ray contribution to Li production implies upper limits on  ${}^6\text{Li}/\text{Li}$  that are lower than the observed  ${}^6\text{Li}/\text{Li}$  in the early Galaxy. These limits are lower than the mean  ${}^6\text{Li}$  abundance suggested by Lemoine et al. (1997), who did not take into account this constraint. As can be seen from equation (29), our upper limit is independent of the absolute values of  $\text{Li}/\text{H}$  and  $\text{Be}/\text{H}$ . If confirmed by further  ${}^6\text{Li}$  observations, and if the observed  $\text{Li}/\text{H}$  around metallicity 0.1 is indeed representative of the average Galactic (protostellar) inventory, this result will require additional  ${}^6\text{Li}$  sources that contribute mainly at low metallicities, for example,  ${}^6\text{Li}$  production by accelerated He before Galaxy formation.

Substituting the lowest  $[Q(\text{Li})/Q(\text{Be})]_{\text{cr}} \simeq 6.1$  (Table 3, model 1 with  $\xi = 0$ , or Figs. 9b and 9c) into equation (28), we obtain

$$M_7 < M_{11} \frac{7}{56} \left( \frac{10}{Z_\odot} \Delta \frac{\text{Li}}{\text{H}} - 6.1 \frac{\text{Be}}{\text{Fe}} \right) \simeq 2.4 \times 10^{-7} M_\odot, \quad (30)$$

where we used  $M_{11} = 0.11 M_\odot$ ,  $\Delta = 0.5$ ,  $\text{Li}/\text{H} \simeq 1.7 \times 10^{-10}$ , and  $\text{Be}/\text{Fe} \simeq 1.6 \times 10^{-6}$  from equation (9). This upper limit is lower than the nominal  $\nu$ -induced  ${}^7\text{Li}$  production of  $4 \times 10^{-7} M_\odot$  given above. Furthermore, the limit assumes only a minimal  ${}^6\text{Li}$  production that leads to a significantly lower Li isotopic ratio than observed (lower dashed line in Fig. 14a). We thus conclude that, unlike the  $\nu$ -produced  ${}^{11}\text{B}$  that seem essential for explaining the B isotopic ratio (§ 3.2), the  $\nu$ -induced  ${}^7\text{Li}$  production is quite small and probably negligible. It should be remembered that the two isotopes are produced differently. Whereas  ${}^{11}\text{B}$  results from the direct spallation of  ${}^{12}\text{C}$ ,  ${}^7\text{Li}$  results from  ${}^3\text{He}$ - ${}^4\text{He}$  fusion, the  ${}^3\text{He}$  being produced from  ${}^4\text{He}$  by the neutrinos. Lack of  ${}^7\text{Li}$  production therefore does not rule out  ${}^{11}\text{B}$  production by neutrinos.

As discussed in § 3.1 the constancy of  $\text{Be}/\text{Fe}$  places upper limits on the contribution of the nonmetallic cosmic rays (SSz) on LiBeB production in the Galaxy. These upper limits are shown by the nonzero values of  $\xi$  in Figure 14, where  $\xi$  is the ratio of the energy content in the metal-poor to metal-rich cosmic rays. The  ${}^6\text{Li}$  observation shown in this figure provides an independent confirmation of these upper limits, although, as can be seen, the error bar is so large that significantly higher values of  $\xi$  would be possible. On the other hand, the upper limit on  ${}^6\text{Li}/\text{Li}$  shown by the solid lines, which is based on the constant value of  $\text{Li}/\text{H}$ , implies more stringent upper limits. We find that  $\xi$  should be less than 16 and 7 for models 1 and 3, respectively, and



essentially zero for model 2. The metal-rich cosmic rays in models 1 and 3 have no He, while there is a significant He abundance for these cosmic rays in model 2.

#### 4. GAMMA-RAY LINE EMISSION

LiBeB production by cosmic rays is accompanied by the production of de-excitation gamma-ray line emission (e.g., Meneguzzi & Reeves 1975). Using the techniques for calculating nuclear gamma-ray line emission described previously (e.g., RKL96), we calculate  $Q(3-7 \text{ MeV})/Q(\text{Be})$ , the ratio of the 3–7 MeV gamma-ray production to the Be production, for the various compositions of Table 2, and for the spectrum of equation (6) with  $s = 2$  and various values of the cutoff energy  $E_0$ . Next we assume that the bulk of the current epoch Be production is due to SNIIs, as it was in the low-metallicity era of the Galaxy. The justification for this assumption is provided by the facts that (i) the solar Be/Fe (e.g., Anders & Grevesse 1989) is lower by about a factor of 2 than the Be/Fe in the low-metallicity era (eq. [9]), and (ii) that only about 50% of the current Fe production is due to SNIIs, indicating that the Type Ia supernovae, which produce most of the other 50% of the Fe, do not produce significant amounts of Be. The 3–7 MeV gamma-ray line emission from the central regions of the Galaxy is then given by (see Ramaty 1996)

$$\Phi(3-7) = \zeta 10^{-46} \frac{Q(\text{Be})}{\text{SNII}} \frac{Q(3-7)}{Q(\text{Be})} \dot{N}_{\text{SNII}} \text{ (photons cm}^{-2} \text{ s}^{-1}\text{)}, \quad (31)$$

where  $0.5 \lesssim \zeta \lesssim 2$  is a parameter that takes into account the spatial distribution of the sources of the nuclear line emission (Skibo 1993),  $Q(\text{Be})/\text{SNII} = 3.8 \times 10^{48}$  atoms is the Be yield per SNII (§ 3.1), and  $\dot{N}_{\text{SNII}}$  is the current rate Type II supernova rate, about three per century (van den Bergh & Tammann 1991).

The results are shown in Figure 15 for the indicated parameters. Also shown are the upper limit on the 3–7 MeV line emission obtained with the *Solar Maximum Mission* (SMM; Harris, Share, & Messina 1995) and the observed total (mostly continuum) 3–7 MeV emission from the

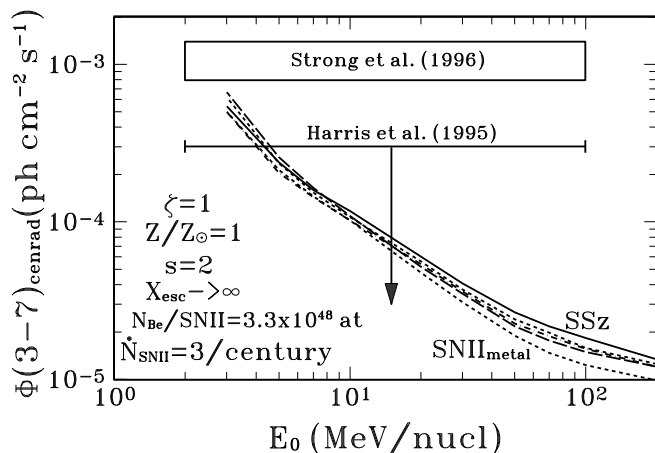


FIG. 15.—Predicted nuclear gamma-ray line fluxes from the central radian of the Galaxy. The calculations assume that all the current era Be production is due to cosmic rays accelerated by SNIIs with a total Be production of  $3.8 \times 10^{48}$  atoms per SNII. The Harris et al. (1995) upper limit is for line emission, whereas the Strong et al. (1996) flux represents total photon emission. We see that the various compositions yield essentially identical results.

central radian with COMPTEL (Strong et al. 1996). We see that the SMM upper limit already rules out Be production by very low energy cosmic rays because, for such cosmic rays, the predicted gamma-ray line emission is not observed. We have shown above that the energetic arguments imply that  $E_0 > 50 \text{ MeV nucleon}^{-1}$  for all models. We thus predict that the 3–7 MeV nuclear line emission from the central radian of the Galaxy should not exceed about  $2.5 \times 10^{-5} \text{ photons cm}^{-2} \text{ s}^{-1}$ , with an error of about a factor of 2. This estimate amounts to only 2% of the total 3–7 MeV emission observed with COMPTEL, pointing to the difficulty in observing nuclear gamma-ray line emission from the central regions of the Galaxy. However, this does not preclude the detection of nuclear gamma-ray lines from localized regions such as Orion (Bloemen et al. 1994, 1997).

#### 5. CONCLUSIONS

1. We have derived the energy in cosmic rays per SNII, averaged over the IMF, that is required to produce the Be. For cosmic rays with energy spectra resulting from acceleration by strong shocks and exponential high-energy cutoffs at energies larger than about  $70 \text{ MeV nucleon}^{-1}$ , the required energy is about  $2 \times 10^{50}$  ergs for a composition similar to that of the current Galactic cosmic rays, and about a factor of 7 lower for cosmic rays containing only metals (C and heavier nuclei) but no H and He. These energetic requirements are quite reasonable for supernovae. In particular, the lower energetic requirements for the compositions without H and He allow models with less available energy for acceleration per SNII (e.g., acceleration by the reverse supernova shock) or models in which only a small fraction of the SNIIs are involved in Be production (e.g., SNIIs from massive star progenitors). However, if the cosmic rays are accelerated out of the ISM, then at a metallicity of  $10^{-3}$ , the required energy is at least  $6 \times 10^{52}$  ergs per SNII, which is nearly 2 orders of magnitude greater than the total available mechanical energy in the ejecta. This result, together with the constancy of Be/Fe as a function of metallicity, rules out cosmic-ray acceleration solely out of the ISM. We thus require the acceleration of metal-rich cosmic rays, presumably freshly nucleosynthesized matter before it mixes into the ISM. The current B and Be data, however, do not allow us to determine whether these metal-rich cosmic rays are predominantly low- or high-energy cosmic rays, although very low energies can be excluded. To further narrow these constraints, we need more accurate measurements of B/Be and the measurement of  $^{11}\text{B}/^{10}\text{B}$  in the early Galaxy, as well as the detection of nuclear gamma-ray lines from sites other than Orion.

2. The energetic requirements for light-element production increase rapidly with decreasing cutoff energies, effectively ruling out models with cutoffs below about  $50 \text{ MeV nucleon}^{-1}$ . If all the Galactic Be is produced by low-energy cosmic rays with such low-cutoff energy, we would predict that the flux of 3–7 MeV nuclear gamma-ray line emission from the central radian of the Galaxy should be about  $2.5 \times 10^{-5} \text{ photons cm}^{-2} \text{ s}^{-1}$  with an error of a factor of 2. The detection of much larger nuclear line fluxes would indicate the presence of sources in which the Be that is produced, together with the gamma rays, is either destroyed in the source region or prevented from escaping from the sources to the ISM.

3. LiBeB production by the high-velocity particles in supernova ejecta can only be responsible for less than a few

tenths of a percent of the total Galactic LiBeB ( ${}^6\text{Li}$ , Be, and B) inventory. Without further acceleration, the energies of these particles are less than about  $10 \text{ MeV nucleon}^{-1}$  and thus very inefficient in producing nuclear reactions. Therefore, any significant contribution to the Galactic LiBeB production would require at least 2 orders of magnitude more energy per SNII than the total energy of the ejecta.

4. It is very difficult to reproduce the meteoritic  ${}^{11}\text{B}/{}^{10}\text{B}$  ratio of  $4.05 \pm 0.2$  (Chaussidon & Robert 1995) by cosmic-ray interactions. Since the energetic arguments rule out very steep, low-energy cosmic-ray spectra, a remaining possibility is an artificial spectrum, essentially flat out to about  $30\text{--}50 \text{ MeV nucleon}^{-1}$  and steeply cut off at higher energies. This strongly suggests that neutrino interactions in SNIIs make an important contribution to the Galactic  ${}^{11}\text{B}$  inventory, alleviating the need for a low-energy cosmic-ray component. We do not reproduce the maximum in  ${}^{11}\text{B}/{}^{10}\text{B}$  as a function of metallicity, and the accompanying maximum in B/Be, caused by the introduction of  ${}^{11}\text{B}$  production by neutrinos (Vangioni-Flam et al. 1996). The variation with metallicity of these ratios is solely the consequence of the assumption that the acceleration of the low-energy cosmic rays is associated mainly with SNIIs from very massive stellar progenitors, whose lifetimes are quite short, while the  ${}^{11}\text{B}$  production by neutrinos results from all SNIIs that, on average, have longer lifetimes. The effects of different lifetimes of the various SNII progenitors should be manifest in the Be/Fe ratio, and there seems to be no evidence for such effects. We find that the yield of neutrino-produced  ${}^{11}\text{B}$  per SNII is in the range  $(2\text{--}7) \times 10^{-7} M_{\odot}$ , with a factor of 2 uncertainty. This range includes the nominal Woosley & Weaver (1995) value of  $6 \times 10^{-7} M_{\odot}$ . Our derived limits follow from the assumption that in the early Galaxy,  ${}^{11}\text{B}/{}^{10}\text{B}$  is at least as high as the meteoritic value and that B/Be does not exceed 34, as suggested by Edvardsson et al. (1994). We also showed that the lower limit on the neutrino contribution implies that  $\text{B/Be} > 16$  in the early Galaxy, a value that seems to require a non-LTE correction for the observed B/Be ratios (Kiselman & Carlsson 1996).

5. The production of  ${}^6\text{Li}$  in  $\alpha\text{--}\alpha$  reactions provides information on metal-poor cosmic rays, such as those that could be accelerated from the ISM. The  ${}^6\text{Li}/\text{Be}$  production ratio can be as low as 2.6 for cosmic rays containing only metals and energy spectra extending to relativistic energies. For a cosmic-ray source composition, which includes He, the  ${}^6\text{Li}/\text{Be}$  production ratio increases to about 6 if the spectrum extends to relativistic energies, but it remains lower than 20 as long as the high-cutoff energy exceeds  $50 \text{ MeV nucleon}^{-1}$ . The  ${}^6\text{Li}/\text{Be}$  production ratio due to cosmic rays accelerated out of the ISM can become very high at low

metallicities, but the contribution of such cosmic rays is limited by the observed linear evolution of Be. These various cosmic-ray  ${}^6\text{Li}/\text{Be}$  production ratios notwithstanding, the most stringent limits on  ${}^6\text{Li}$  production in the early Galaxy come from the constancy of Li/H up to a metallicity of about 0.1. Because  ${}^6\text{Li}$  is expected to evolve as fast as Be, the observed constancy of Li/H limits the Li isotopic ratio ( ${}^6\text{Li}/\text{Li}$ ) at metallicities around 0.01 to values marginally lower than those observed. This suggests the existence of  ${}^6\text{Li}$  sources that contribute mainly at low metallicities. The Li production by metal-poor cosmic rays can be used to set limits on the ratio of the energy contained in such cosmic rays to those in the metal-rich cosmic rays that produce the Be and part of the B. For models 1 and 3 in Table 3, this ratio should not exceed 16 and 7, respectively, and should vanish for model 2. The metal-rich cosmic rays in models 1 and 3 have no He, while there is a significant He abundance for these cosmic rays in model 2. Our limit on the contribution of neutrino-induced nucleosynthesis to  ${}^7\text{Li}$  production in SNIIs is lower by about a factor of 2 than the nominal Woosley & Weaver (1995) value.

*Note added in manuscript.*—After the completion of this paper, Duncan et al. (1997) presented results on B/Be for nine stars. Their average non-LTE ratio is  $15 \pm 3$ . While they point out that uncertainties in the non-LTE correction may affect this result, we note that if  ${}^{11}\text{B}/{}^{10}\text{B} = 4$ , as required by meteoritic data, this low B/Be is inconsistent with accelerated particle production of B and Be, even if  $E_0$  is allowed to be very low (i.e., very low energy cosmic rays). On the other hand,  ${}^{11}\text{B}/{}^{10}\text{B} = 4$  can be achieved with our lowest accelerated particle-produced  $\text{B/Be} = 10$  (Fig. 4a), the associated  ${}^{11}\text{B}/{}^{10}\text{B} = 2.2$  (Fig. 6b), and a 37% contribution from neutrinos to the total B production. Using equation (22), we obtain a total  $\text{B/Be} = 16$  that is consistent with the Duncan et al. (1997) range. This result also can be seen in Figure 13a, where for  ${}^{11}\text{B}/{}^{10}\text{B} = 4$ , at the highest  $E_0$ ,  $\text{B/Be} = 16$  and  $\text{B/Be} < 20$  for  $E_0 > 100 \text{ MeV nucleon}^{-1}$ . Thus, if  ${}^{11}\text{B}/{}^{10}\text{B} = 4$  in the early Galaxy, the low B/Be measured by Duncan et al. (1997) can be best understood if the cosmic rays are predominantly of high energies and there is substantial additional production of  ${}^{11}\text{B}$  by neutrinos.

We acknowledge W. Webber, D. Mercer, and S. Austin for supplying us with cross section data prior to publication, D. Hartmann, W. Haxton, and G. Wallerstein for illuminating discussions on neutrino interactions in supernovae and Li production in asymptotic giant branch stars, M. Lemoine for the useful exchange of information on  ${}^6\text{Li}$ , and V. Tatischeff for carefully reading the manuscript. We also acknowledge support from NASA's Astrophysics Theory Program.

## REFERENCES

- Anders, E., & Grevesse, N. 1989, *Geochim. Cosmochim. Acta*, 53, 197  
 Barkas, W. H., & Berger, M. J. 1964, *Tables of Energy Losses and Ranges of Heavy Charged Particles* (SP-3013; Washington, DC: NASA)  
 Bloemen, H., et al. 1994, *A&A*, 281, L5  
 ———, 1997, *ApJ*, 475, L25  
 Cassé, M., Lehoucq, R., & Vangioni-Flam, E. 1995, *Nature*, 373, 318  
 Casuso, E., & Beckman, J. E. 1997, *ApJ*, 475, 162  
 Chaussidon, M., & Robert, F. 1995, *Nature*, 374, 337  
 Cowsik, R., & Friedlander, M. 1995, *ApJ*, 444, L29  
 Digel, S. W., Hunter, S. D., & Mukherjee, R. 1995, *ApJ*, 441, 270  
 Duncan, D. K., et al. 1996, *PASP*, 99, 179  
 Duncan, D. K., Lambert, D. L., & Lemke, M. 1992, *ApJ*, 401, 584  
 Duncan, D. K., Primas, F., Rebull, L. M., Boesgaard, A. M., Deliyannis, C. P., Hobbs, L. M., King, J. R., & Ryan, S. G. 1997, *ApJ*, 488, 338  
 Edvardsson, B., et al. 1994, *A&A*, 290, 176  
 Ellison, D. C., & Ramaty, R. 1985, *ApJ*, 298, 400  
 Engelmann, J. J., et al. 1990, *A&A*, 233, 96  
 Federman, S. R., Lambert, D. L., Cardelli, J. A., & Sheffer, Y. 1996, *Nature*, 381, 764  
 Fields, B. D., Cassé, M., Vangioni-Flam, E., & Nomoto, K. 1996, *ApJ*, 462, 276  
 Fields, B. D., Olive, K. A., & Schramm, D. N. 1994, *ApJ*, 435, 185  
 ———, 1995, *ApJ*, 439, 854  
 Garcia-Munoz, M., et al. 1987, *ApJS*, 64, 269  
 Grevesse, N., Noels, A., & Sauval, A. J. 1996, in *ASP Conf. Ser. 99, Cosmic Abundances*, ed. S. E. Holt & G. Sonneborn (San Francisco: ASP), 117  
 Harris, M. J., Share, G. H., & Messina, D. C. 1995, *ApJ*, 448, 157  
 Hernanz, M., José, J., Coc, A., & Isern, J. 1996, *ApJ*, 465, L27  
 Hobbs, L. M., & Thornburn, J. A. 1994, *ApJ*, 428, L25  
 Kiselman, D., & Carlsson, M. 1996, *A&A*, 311, 680

- Kozlovsky, B., Ramaty, R., & Lingenfelter, R. E. 1997, *ApJ*, 484, 286
- Lemoine, M., Schramm, D. N., Truran, J. W., & Coppi, C. J. 1997, *ApJ*, 478, 554
- Lingenfelter, R. E. 1992, in *The Astronomy and Astrophysics Encyclopedia*, ed. S. P. Maran (New York: Van Nostrand), 139
- Lund, N. 1989, in *Cosmic Abundances of Matter*, ed. C. J. Waddington (New York: AIP), 111
- Meneguzzi, M., Audouze, J., & Reeves, H. 1971, *A&A*, 15, 337
- Meneguzzi, M., & Reeves, H. 1975, *A&A*, 40, 91
- Mercer, D. J., Austin, S. M., & Glagola, B. G. 1997, *Phys. Rev. C*, 55, 946
- Meyer, J.-P., Drury, L. O'C., & Ellison, D. C. 1997, *ApJ*, 487, 182
- Mitler, H. E. 1972, *Ap&SS*, 17, 186
- Pierce, T. E., & Blann, M. 1968, *Phys. Rev.*, 173, 390
- Plez, B., Smith, V. V., & Lambert, D. L. 1993, *ApJ*, 418, 812
- Prantzos, N. 1993, in *Nuclei in the Cosmos*, ed. F. Kappeler & W. Wisshak (Bristol: IOP), 471
- Prantzos, N., Cassé, M., & Vangioni-Flam, E. 1993, *ApJ*, 403, 630
- Ramaty, R. 1996, *A&AS*, 120, C373
- Ramaty, R., Kozlovsky, B., & Lingenfelter, R. E. 1995, *ApJ*, 438, L21
- . 1996, *ApJ*, 456, 525 (RKL96)
- Ramaty, R., Kozlovsky, B., Lingenfelter, R. E., & Reeves, H. 1997a, in *ASP Conf. Ser., The Scientific Impact of the Goddard High Resolution Spectrograph*, ed. J. C. Brandt, T. B. Ake, & C. C. Peterson (San Francisco: ASP), in press
- Ramaty, R., Reeves, H., Lingenfelter, R. E., & Kozlovsky, B. 1997b, *Nucl. Phys. A*, in press
- Read, S., & Viola, V. 1984, *At. Data Nucl. Data Tables*, 31, 359
- Reeves, H. 1994, *Rev. Mod. Phys.*, 66, 193
- Reeves, H., Fowler, W. A., & Hoyle, F. 1970, *Nature Phys. Sci.*, 226, 727
- Reeves, H., & Prantzos, N. 1995, in *The Light Element Abundances*, ed. P. Crane (Berlin: Springer), 382
- Silk, J. 1995, *ApJ*, 438, L41
- Skibo, J. G. 1993, Ph.D. thesis, Univ. Maryland
- Smith, V. V., Lambert, D. L., & Nissen, P. E. 1993, *ApJ*, 408, 262
- Spite, F., & Spite, M. 1993, in *Origin and Evolution of the Elements*, ed. N. Prantzos, E. Vangioni-Flam, & M. Cassé (Cambridge: Cambridge Univ. Press), 201
- Strong, A. W., et al. 1996, *A&AS*, 120, C381
- Timmes, F. X., Woosley, S. E., & Weaver, T. A. 1995, *ApJS*, 98, 617
- Truran, J. W., & Timmes, F. X. 1994, in *Nuclei in the Cosmos III*, ed. M. Busso, R. Gallino, & C. M. Raiteri (New York: AIP), 501
- van den Bergh, S., & Tammann, G. A. 1991, *ARA&A*, 29, 363
- Vangioni-Flam, E., Cassé, M., Fields, B. D., & Olive, K. A. 1996, *ApJ*, 468, 199
- Walker, T. P., et al. 1993, *ApJ*, 413, 562
- Wallerstein, G., & Morell, O. 1994, *A&A*, 281, L37
- Webber, W. R., Kish, J. C., & Schrier, D. A. 1990a, *Phys. Rev. C*, 41, 520
- . 1990b, *Phys. Rev. C*, 41, 547
- Woosley, S. E., Hartmann, D. H., Hoffman, R. D., & Haxton, W. C. 1990, *ApJ*, 356, 272
- Woosley, S. E., Langer, N., & Weaver, T. A. 1993, *ApJ*, 411, 823
- Woosley, S. E., & Weaver, T. A. 1995, *ApJS*, 101, 181